



POLITECNICO DI TORINO

MASTER DEGREE IN BIOMEDICAL ENGINEERING

**Channel Selection for Proportional
Myoelectric Control of a Lower Limb
Exoskeleton by Using Linear Regression
Technique and High Density sEMG**

Candidate:

Niccolò ROSSO

Supervisors:

Prof. Marco GAZZONI

Prof. Dario FARINA



Imperial College
London



July 26 2018

POLITECNICO DI TORINO

Abstract

Department of Mechanical and Aerospace Engineering (DIMEAS)

Master degree

Channel Selection for Proportional Myoelectric Control of a Lower Limb Exoskeleton by Using Linear Regression Technique and High Density sEMG

by Niccolò ROSSO

Objective. Recent studies have shown the possibility to achieve a proportional myoelectric control of a lower limb exoskeleton for rehabilitation using a regression-based approach, but optimal channel selection has been little investigated. In this study the feasibility to localize the most informative channels to extract a proportional simultaneous myoelectric control for a multi degrees of freedom exoskeleton has been examined. *Approach.* Five able-bodied subjects took part in this study, which was divided in two experiments. High density surface electromyographic (sEMG) signals were recorded with electrodes grids in both parts of this study. In details, four grids of 8x4 electrodes and three grids of 8x8 electrodes have been used. Angle signals were recorded with two electrogoniometers only in the second experiment. In the first experiment, subjects performed ankle and knee movements separately (dorsiflexion/plantarflexion of the ankle, flexion/extension of the knee). In the second part of this study, subjects performed movements with combinations of the two DoFs. Channel selection was performed in the first experiment by least absolute shrinkage and selection operator (LASSO) method. In both experiments, angles were estimated from EMG features with ridge regression model using channel subsets selected by LASSO. *Main results.* Channel selection performed by LASSO proved to be robust in terms of channel subsets chosen and training data reduction. Performances obtained in angle reconstruction using complete configurations can be retained or even overcome with the smallest configurations (3 channels for ankle, and 4 channels for knee). *Significance.* From analysis results, it is possible to conclude that LASSO implements an effective and robust channel selection for natural, accurate and proportional control. We expect that our results will provide a useful guideline to select most informative channels for the extraction of a proportional and simultaneous myoelectric control of a rehabilitation exoskeleton for lower limb.

Contents

Abstract	i
1 Introduction	1
1.1 Electromyography signal	2
1.2 Regression-based approach	4
2 Thesis aim	5
3 Materials and methods	6
3.1 Experimental procedure	6
3.1.1 First experimental procedure: single joint	7
3.1.1.1 Ankle	7
3.1.1.2 Knee	8
3.1.2 Second experimental procedure: two joints	9
3.2 Data collection and instrumentation	11
3.3 First experimental procedure setup	13
3.3.1 Electrodes grids	13
3.3.2 Electrogoniometers	15
3.4 Second experimental procedure setup	16
3.5 Data analysis	17
3.5.1 Preprocessing	17
3.5.2 Feature extraction	17
3.5.3 Regression model	17
3.5.4 Nested cross validation	18
3.6 Channel selection	20
3.6.1 Lasso	20
3.7 Training data reduction	21
3.8 Robustness test	21
3.8.1 IED evaluation	21
3.8.2 Subsets weight homogeneity	21

3.8.3	Overlap ratio	22
3.9	Angles decoding	23
4	Results	24
4.1	First experiment results	24
4.1.1	Impact of reduced training data	24
4.1.2	Robustness test	27
4.1.2.1	Consistency of electrode selection	27
4.1.2.2	Subsets weight homogeneity	31
4.1.2.3	Overlap ratio	33
4.1.3	Channel configurations obtained by Lasso	37
4.1.3.1	Ankle channel configuration analysis	40
4.1.3.2	Knee channel configuration analysis	43
4.2	Second experiment results: angle reconstruction	46
4.2.1	Ankle	47
4.2.2	Knee	50
4.2.3	Statistical analysis	53
5	Conclusion	54
	Bibliography	56

Chapter 1

Introduction

Electromyographic (EMG) signals of residual muscles have been widely involved to control electrically powered upper and lower limb prostheses, because they have enough information about muscular activity. Indeed, an enormous number of people lost their limbs in various accidents or they are born without one or more limbs. So far, many studies focused on pattern recognition based approach to control prostheses, and many progresses have been made in improving classification accuracies and in distinguishing different emg patterns. Despite high performances and robustness issues have been reported, most of pattern recognition based myoelectric prostheses demonstrated a crucial limitation in practical use in only one degree of freedom can be controlled at time [8]. Recent works tried to extend classification to more movements at same time and to discriminate combined motions but they still limit type of movements not allowing an independent proportional control. Conversely, natural movement can be reproduced only using independent and proportional control. This type of control can be achieved with regression technique. The major difference between classification and regression is that regressor does not decide for a certain class but provides a continuous output command for multiple DoFs, therefore become possible a more intuitive and natural control of myoelectric prostheses [5]. This need values not only for prostheses but also for exoskeleton, indeed both cases there is a need to decode independent proportional and simultaneous control of more DoFs. Robotic exoskeleton aims to rehabilitate and restore a movement in subject that are not able to perform because of paraplegia or spinal cord injury (SCI). Recovery of lower limb function after these injuries is fundamental to improve quality of life and independence of this people. Generally muscles of this population are weak or paralyze, thus they are not able to provide necessary activation to promote movements. For this reason, combined strategy has been developed to provide external support during movement wearing exoskeleton such as Functional Electrical Stimulation (FES) [1]. Rehabilitation procedure for people with these muscular issues is complicated because extents, position and causes of muscular damages are patient specific, for this reason

there is a need to locate and evaluate most informative areas of each muscle in order to optimize rehabilitation procedure. Consequently, number of electrodes to acquire emg signals is reduced and computational time benefits of this reduction: real time system based are necessary to secure patient during rehabilitation procedure.

Regardless the strategy to exploit regression or classification, and type of prostheses or exoskeleton the first step in implementation of myoelectric control is to select an appropriate number of electrodes and their optimal sites. As far as concern pattern recognition based myoelectric control, channel selection has been widely investigated; but to our best knowledge a few studies examined the impact of channel selection on regression base myoelectric control [14], [5]. Generally, performances in control degraded reducing number of electrodes, hence an important step toward clinical use is to find a method that perform well with a small number of electrodes [9]. Since in term of clinical application a method requires short time for the setup and little user training, the goal of this study is to identify the best configurations of electrodes to obtain a simultaneous proportional myoelectric control of two degrees of freedom. Linear regression model has been used in this work to extract a control signal from ankle and knee joint in order to drive a lower limb exoskeleton. In the last part of the study, angles sensors were used only to evaluate the performances of the approach. The study is divided in two experiments that are described in the following chapters.

1.1 Electromyography signal

The electromyography (EMG) signal is a manifestation of electric potential field due to the depolarization of the sarcolemma which is the outer membrane of muscle fiber. To detect it, intramuscular or surface electrodes are positioned on a certain distance from the sources. The tissue inserted between electrodes and source acts as so called volume conductor which is responsible for the features of the recorded signals, particularly for what concern its frequency content and distance up to which can be detected. In intramuscular recordings, because electrodes are positioned very closely to the source the effect of tissue is generally small. On the contrary, for surface detection the volume conductor acts as low-pass filtering on emg signal [13].

Potential generated on muscle fiber is the emg source. In detail, when an electric impulse propagating along motoneuron arrives at nerve terminal produces electrochemical phenomenon that generates a depolarization zone, and the potential gradient propagates along muscles fibers from neuromuscular junction to tendons. Potential due to activation of a single motor unit is called motor unit action potential (MUAP). The action potential propagates with a certain velocity that depends on type and fiber diameter, this velocity

is called conduction velocity (CV). A schematic representation of what described is reports in figure 1.1 (a) and (b). In surface electromyography, when emg signal is recorded by monopolar detection it is affected by common mode components that causes interferences (for example power line) and also by low pass filtering effect of the tissue. To compensate these drawbacks emg signals are detected as linear combination of signals acquired from different electrodes, the simplest procedure is the bipolar montage which can be seen as spatial filtering of monopolar surface emg signal [13].

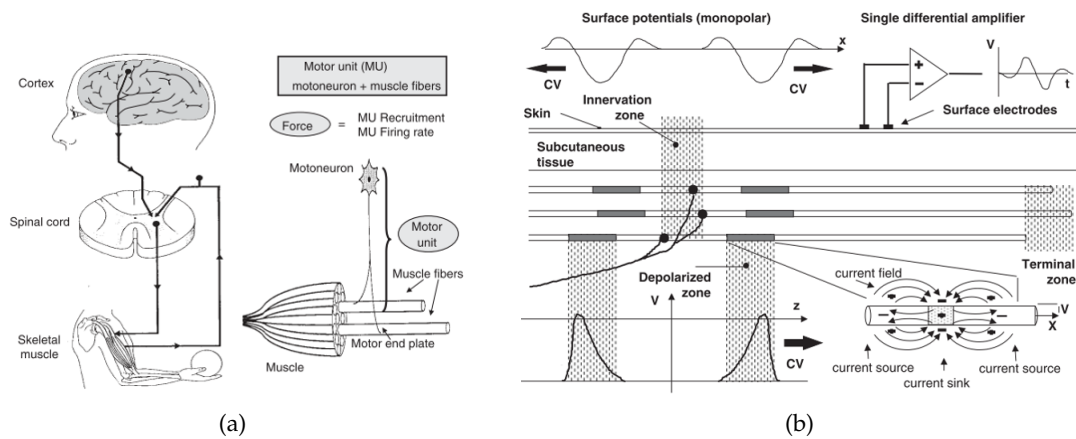


FIGURE 1.1: (a) Motor control mechanism of Motor Unit which is made of α -motoneuron in spinal cord and the fibers of muscles innervated. (b) Propagation of motor unit action potential. From innervation region of any fiber, two depolarization zones propagate to limit of each fiber. Because of differences in innervation region, electric field sources are not perfectly aligned under recording electrodes. Therefore, the summation of all these contributions (MUAP) produce the resultant signal[13].

1.2 Regression-based approach

Regression-based approach estimates a continuous and multivariate outputs comprising all DoFs simultaneously [4]. This allows an independent simultaneous and proportional control which results more natural and fluent, providing a better estimation. On the contrary, classification based approach decides for a specific class therefore there is a lack of this natural control [11]. Regression-based approach combined with real time feedback permits intuitive correction by the user. Since small variation in emg signal causes variation in the output system, user getting the feedback can modify contraction pattern in a intuitive way.

Data labels are required with emg data to train a regressor, several studies used torque or forces of the corresponding DoFs to obtain labels, but it also possible to use joint angles despite of forces for training [10]. In this study, the feasibility of extracting a robust control signal using regression based approach providing angular labels will be investigated.

Chapter 2

Thesis aim

At Neuro-rehabilitation Engineering Laboratory of Imperial College, researchers make studies on proportional and simultaneous myoelectric control of multiple degrees of freedom prosthesis for upper limb. Recently, they conducted studies about EMG-driven model based of multi-joint exoskeleton system for lower limb, joints of interest were ankle and knee. Indeed, degrees of freedom took into account in this work are two: one for each joint. Most of Exoskeleton structures are bulky and for this reason are not suitable for many electrodes grids and sensors placement on the subject skin. Therefore, there is a need to localize most informative regions of each muscles in order to place on them only a small number of electrodes. The aim of this study is to verify the feasibility to reduce number of electrodes needed to compute joint angular movements, without using angles sensors, in order to extract a proportional myoelectric control for two degrees of freedom exoskeleton.

Channels selection method used in this study is least absolute shrinkage and selection operator (LASSO), which is an efficient regularization method for high dimensional regression [15]. Lasso is widely used for subset selection because it produce some coefficients of linear regression exactly zero and hence it provides interpretable models. In this work, lasso is used only to select bipolar emg channels, then the regression model of the selected channel subsets is made using ridge regression method [8].

This was a preliminary study, therefore it was carried out only with healthy able-bodied subjects, without wearing exoskeleton. This work was divided in two experiments, then data were all acquired and then processed. During experiments, monopolar high density surface emg signals were recorded using by electrodes grids placed on specific muscles of knee and ankle. Control signal, that was extracted from a limited number of channels for each joint, is an angular signals that estimated the angles performed by joint during the task. In order to evaluate these estimation, control signal for ankle and knee were compared to angular signals recorded using electrogoniometers. All data were acquired only from the right lower limb of the subjects.

Chapter 3

Materials and methods

3.1 Experimental procedure

Five healthy able-bodied subjects took part in this study which was divided in two parts. Subjects were asked to move their leg and ankle following trapezoidal trajectories provided on the screen (figure 3.1). In both experiments on line feedback is provided to the subject during the task, red dots were drawn on the trajectory to temporize movements, furthermore patients is verbally encouraged and guided when necessary. The time used for the cue was 30s: the first, the middle the last horizontal segment of the cue last about 5s and correspond to the maintenance of reference position, the other segments corresponding to 'flexion', 'extension' and 'hold' labels last about 3s. The reference position and movements of flexion and extension depends on the joint and are explained in details in section 3.1.1.1 and 3.1.1.2. In both experiments data were obtained from right lower limb of each subject.

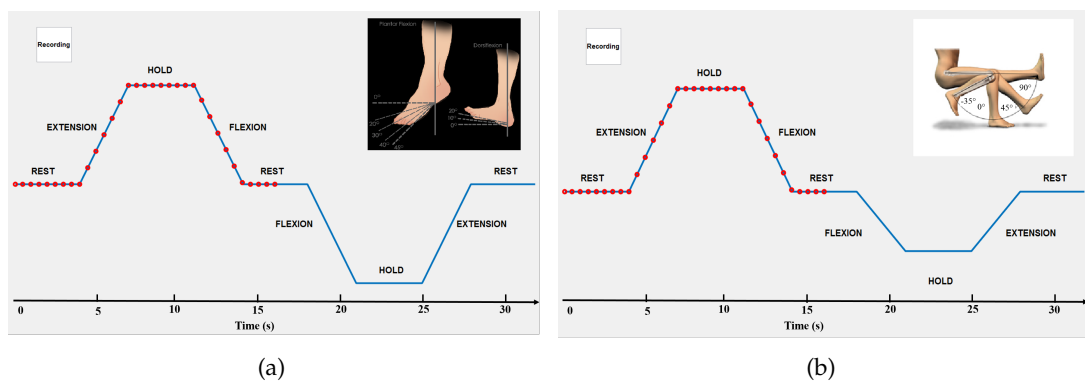


FIGURE 3.1: Target trajectories provided to subjects as visual feedback during (a) ankle and (b) knee movements.

3.1.1 First experimental procedure: single joint

The purpose of the first experiment is to realize an effective channels selection, that is to find the subset of channels that better allows to reconstruct joint angles. In this first part of the study angular signals were not recorded, only emg signals were acquired. Subjects were required to follow a target trajectory on a screen. Ankle and knee joint were evaluated separately, and for each joint emg signals corresponding to 10 repetitions of the same movements were recorded. Therefore channel subsets were selected for ankle joint and then for the knee joint.

3.1.1.1 Ankle

Subjects were set on a chair with fully contact between foot and floor. Subjects performed 10 times movement with 1 DOF, namely plantarflexion and dorsiflexion of the ankle, following the cue provided on a screen (figure 3.1(a)). In the reference position (rest position) of the ankle joint the right foot is in complete contact with floor. As shown in figure 3.1(a), the reference position correspond to the horizontal segments of the trapezoidal cue with label 'rest'. Ascendant and descendant segments correspond to plantarflexion and dorsiflexion phase, whereas in the hold phase the subject kept the position reached in plantarflexion or dorsiflexion. Angles found in literature associated with rest, complete dorsiflexion (first hold phase) and complete plantarflexion (second hold phase) phase are respectively: 0, 30, -50 degree. Figure 3.2 shows movements described.

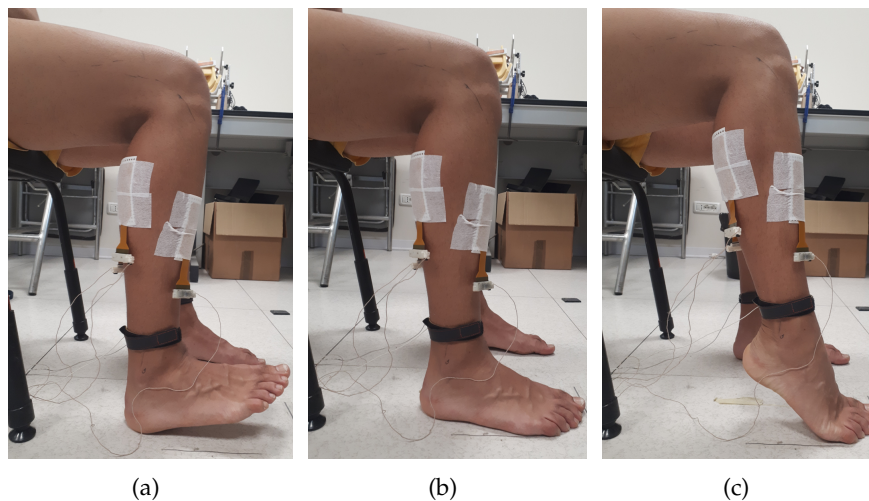


FIGURE 3.2: Ankle joint: (a) dorsiflexion and (b) rest position (c) plantarflexion performed by subject 2.

3.1.1.2 Knee

Subjects were set on a physiotherapy table, in this situation there were no contact between foot and floor. As with the ankle, 10 repetitions of movement with 1 DOF, namely flexion and extension of the knee, were recorded. In the reference position, horizontal segment with label 'rest', the leg was vertically aligned with the table legs (see figure 3.3 (b)), whereas ascendant and descendant phase are related to flexion and extension of the leg. At the end of these phases subject kept the the position reached in complete flexion and extension (figure 3.1(b)). Angles found in literature associated with reference position, leg extension (first hold phase) and leg flexion (second hold phase) phase are respectively: 0, 90,-35 degree. Figure 3.3 shows movements described above.

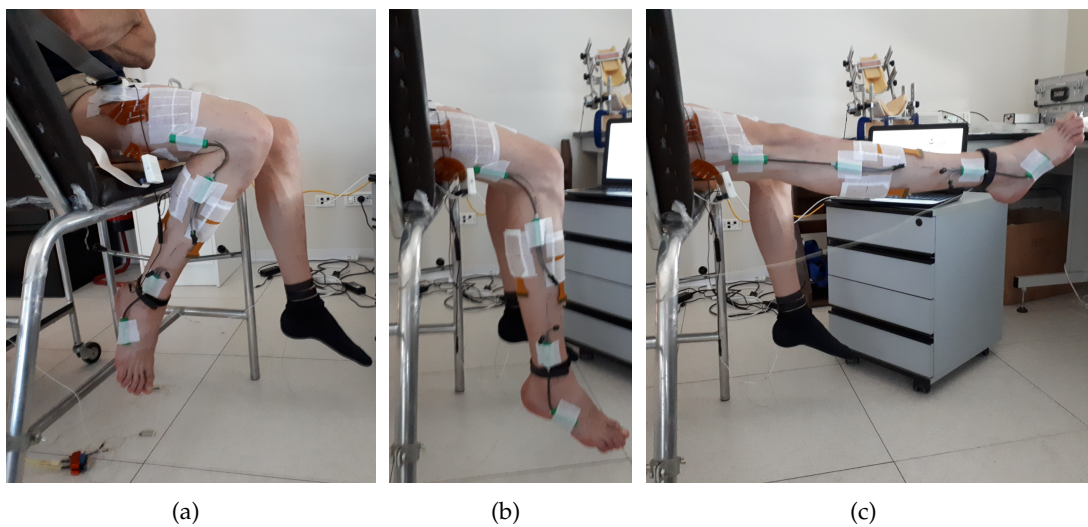


FIGURE 3.3: *Knee joint: (a) leg flexion, (b) rest position and (c) leg extension performed by subject 4.*

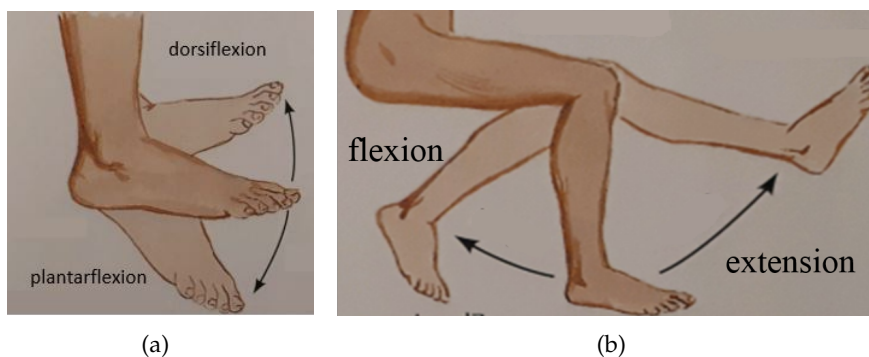


FIGURE 3.4: *Physiological movements for the (a) ankle and (b) knee joint.*

3.1.2 Second experimental procedure: two joints

The aim of this experiment is to evaluate the feasibility of decoding angles signals using a reduced number of electrodes without motion sensors. But to prove it, there is a need of a comparison between angles estimated and real angles provided by a motion sensor. For this reason angles signals were recorded from both joints simultaneously by electrogoniometers, and they are reconstructed using by channel subsets found in the previous experiment (section 3.9). In contrast to first experiment, emg signals were acquired from both joints simultaneously.

The protocol realized in this part of the experiment allowed to appreciate and evaluate emg and angle signals from both joints together, indeed movements with 2 DoFs have been performed. Number of task repetitions recorded was 10. Subjects were set on a physiotherapy table, and an elastic bend has been applied to generate plantar flexion movement coherently with the first experiment. Figure 3.11 shows the complete setup. In this part of the experiment, pilots study pointed out the presence of an offset about angular position relative to reference position (rest position) of both joints. Because legs of subject were not perfectly aligned along vertical direction and although the presence of the elastic bend, sole of right foot is not parallel to the floor. For these reason before processing data in first experiment, these offsets are calculated for ankle and knee of each subject and then eliminated. In this part of the study subjects were asked to follow knee cue and then perform movements as in section 3.1.1.2, but furthermore they were required to combine ankle movements of dorsiflexion and plantarflexion during plateau phase of knee cue. In the ascendant e descendant segments of the trajectory, subjects were free to move the ankle in the way that made them comfortable. As shown in figure 3.5 this second experiment is structured as follow:

- *phase (1)*: ankle and knee joint are in rest position;
- *phase (2)*: from (1) to (2) subject is required to perform extension of knee till reaching maximum extension range (2), at this point subject performs dorsiflexion of the ankle during all duration of this phase. Once finished, subject returns leg in rest position;
- *phase (3)*: leg is in rest position and subject performs plantarflexion of the ankle. At the end of this phase, subject starts to perform knee flexion and ankle is keeping in freely position till phase (4);
- *phase (4)*: at the begin of this phase, subject reaches the maximum flexion of the knee, and then he starts acting a dorsiflexion of the ankle;

- *phase (5)*: from the end of phase (4) subject moves leg and ankle joint to the rest position.

In particular, focusing on phase (2), (3) and (4) and comparing knee and ankle frames is possible to appreciate the movement of dorsiflexion and plantarflexion of the ankle joint.

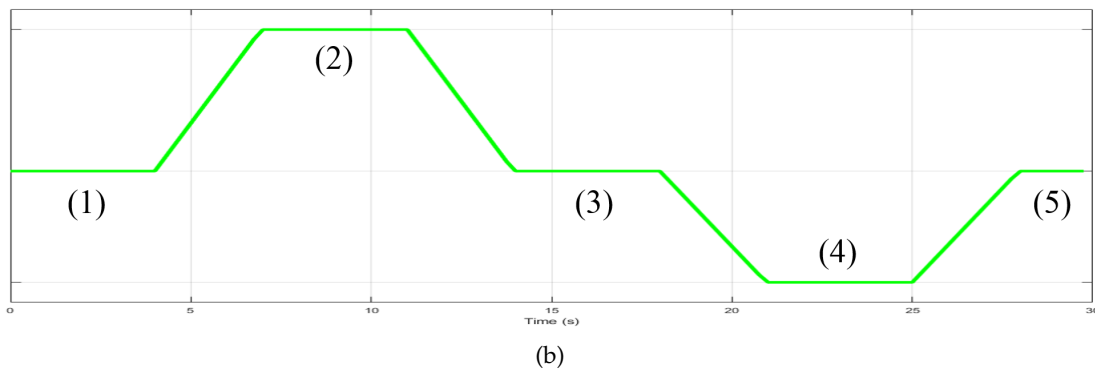
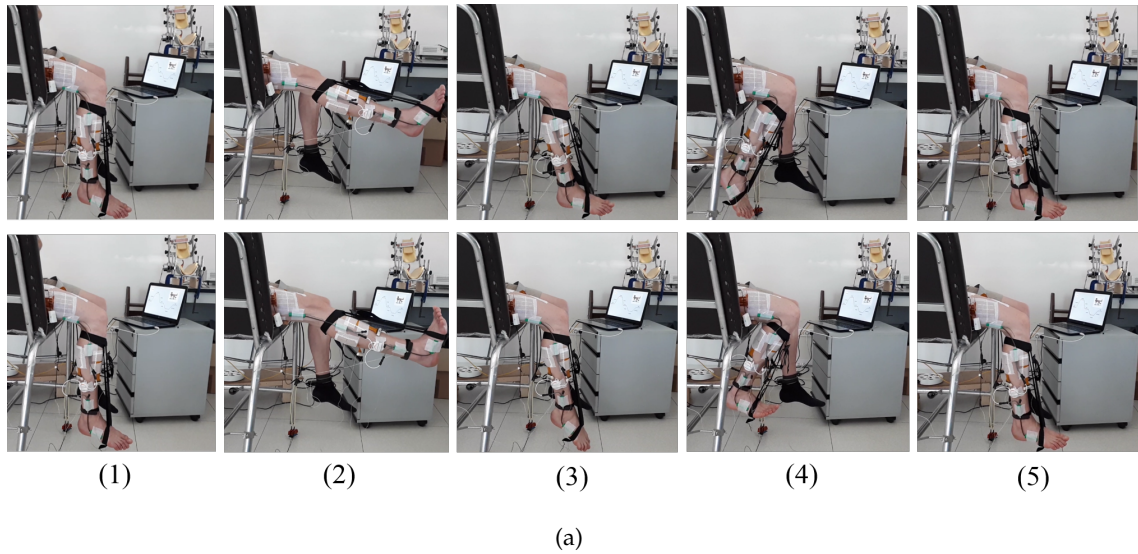


FIGURE 3.5: For a more intuitive visualization of this experiments two rows of frames are reported in (a): first and second row contains frames about main phases movement of knee and ankle, respectively. The same phase are localized along generic target trajectory displayed in (b). Phase 1 and 5 shows both joints in rest position, phase 2 extension of knee and dorsiflexion of ankle, phase 3 rest position of knee and plantarflexion of ankle and phase 4 shows knee flexion and ankle dorsiflexion.

3.2 Data collection and instrumentation

During the experiments monopolar emg signals were detected using high-density (HD) electrodes grids of two different size (figure 3.6): 8x4 and 8x8 (Lisin, OT-Bioelettronica, 10 mm inter-electrode distance (IED)) and acquired using a multichannel amplifier for bioelectrical signals (OT-Bioelettronica, Quattrocento, Turin; 16 bit, sampling frequency 2048 Hz). Patient reference connector has been connected to the right ankle of the subject using a wet strip. Twin-axis electrogoniometers (Biometrics Ltd) have been used to record angle signals from the joints of interest: ankle and knee (figure 3.6). Seeing as how only one DOF along sagittal plane has been studied for each joint, only one axis of the electrogoniometers has been used for each joint. Angles signals were sampled at 2048 Hz by general purpose bluetooth device (OT-Bioelettronica DuePro, Turin). Acquisition devices described are shown in figure 3.7(a) and 3.7(b).

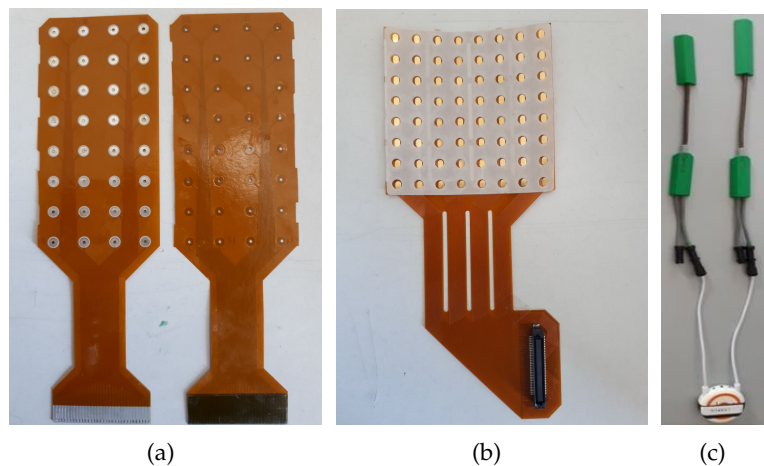


FIGURE 3.6: Figure shows electrodes grids (a) 8x4, (b) 8x8 and (c) electrogoniometers: SG150 for knee (on the right) and SG100 for the ankle (on the left). Electrogoniometers are connected to DuePro device.



FIGURE 3.7: (a) Quattrocento amplifier and (b) DueStation with DuePro device.

Synchronization between emg and angular signals was performed online sending data recorded from DuePro to two auxiliary inputs channels of Quattrocento via DuePro Station, which works as bluetooth token. Graphical User Interface (GUI) realized in MATLAB[®] allowed to evaluate monopolar emg online and to start acquisition of both signals. While subject performed a task following the trajectory on a screen, signals have been controlled on laptop monitor: emg using GUI whereas angles by DuePro software. This allowed to monitor completely the experiment and to stop it when problem occurs. Figure 3.8 shows the complete acquisition system used in this study.



FIGURE 3.8: Acquisition system used in this study.

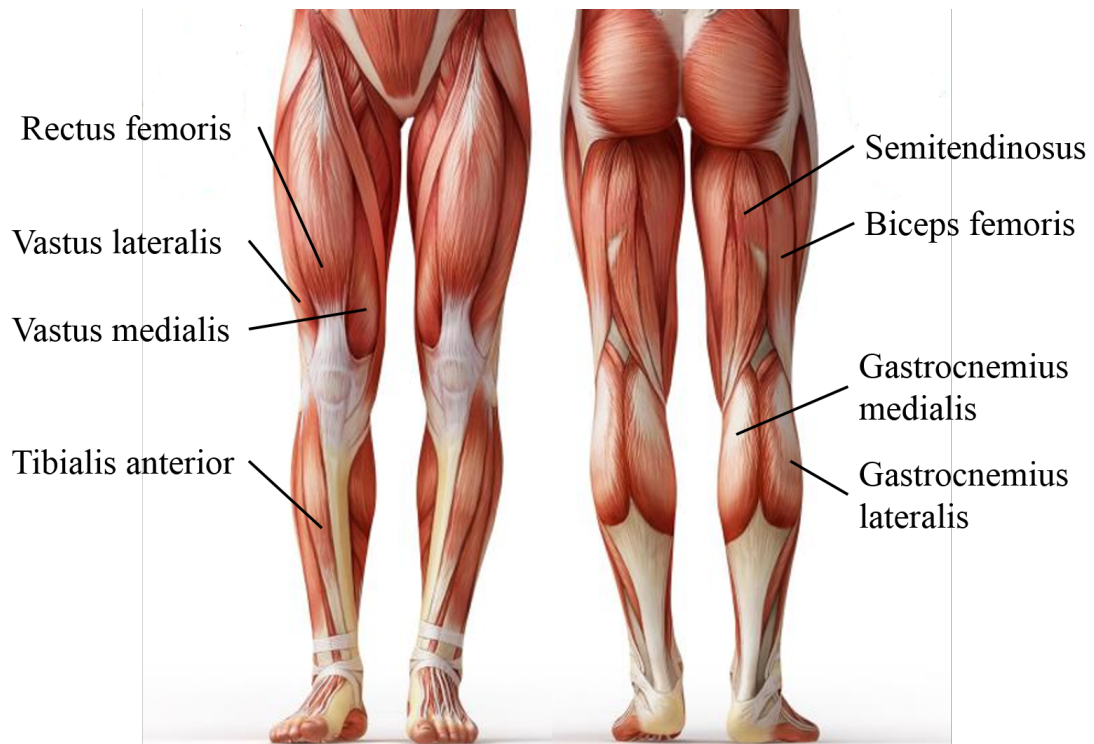
3.3 First experimental procedure setup

3.3.1 Electrodes grids

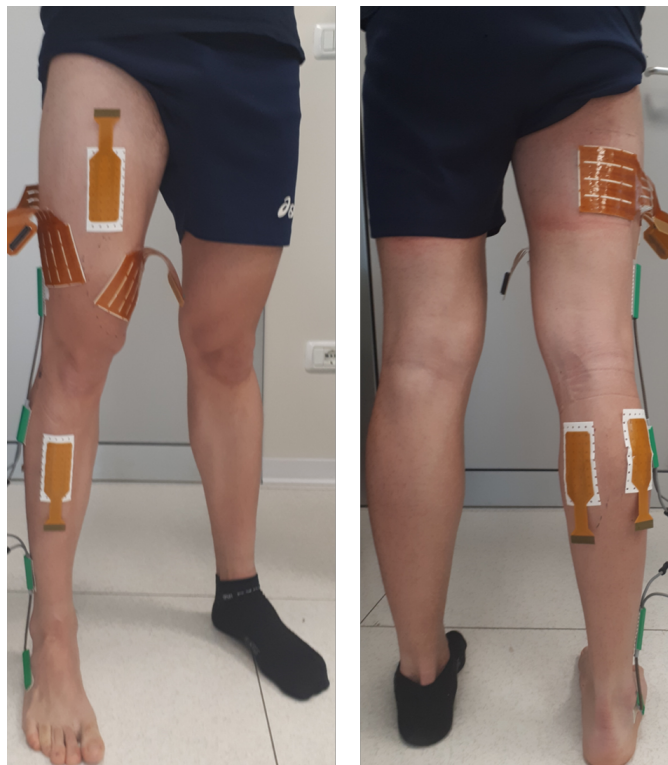
In order to evaluate emg signals of the two joints separately, electrodes grids have been applied in two different times: at first on muscles working on the ankle, and secondly on the muscles of knee. In both cases muscles were located palpating the skin and with the help of an anatomy atlas. During this, subjects were requested to keep the anatomical neutral position and to perform particular movements to identify muscles of interest. Anatomical reference has been reported in figure 3.9 (a) for more intuitive understanding of the placement. Different size electrodes grids were mounted depending on muscles joint:

- *ankle joint*: 8x4 grids have been used with tibialis anterior (TA), gastrocnemius medialis (GM), gastrocnemius lateralis (GL) (figure 3.9). Choice of these muscles is accounted for type of movements of ankle: dorsiflexion and plantarflexion. Indeed, tibialis anterior is responsible for dorsiflexion and gastrocnemius medialis and lateralis are appointed of plantarflexion. 96 was the electrodes number dedicated to muscles of the ankle;
- *knee joint*: 8x4 grids were placed on rectus femoris (RF), whereas 8x8 on vastus lateralis (VL), vastus medialis (VM) and biceps femoris (BF). Semitendinosus muscle has been already recorded with biceps femoris due to the size of the grid used (figure 3.9). Rectus femoris, vastus lateralis and medialis are responsible for knee extension, whereas biceps femoris for knee flexion. 224 were the electrodes placed on muscles of knee.

When recordings about ankle were finished, grids were placed on knee meanwhile grids on ankle were disconnected from the acquisition system but not removed from the subject. This protocol has been preferred instead of placing all electrodes grids since the beginning, this to make the subject more comfortable and to preserve the attachment of the grids, particularly for the 8x8 which are heavier than 8x4.



(a)



(b)

FIGURE 3.9: Anatomical image is reports in (a) to show position and shape of muscles studied. Electrodes grids placement for ankle and knee joint are shown in (b), anterior and posterior view are reported in both images. Grids were attached on tibialis anterior, gastrocnemius medialis, gastrocnemius lateralis for ankle joint and on vastus lateralis, rectus femoris, vastus medialis and biceps femoris for knee joint.

3.3.2 Electrogoniometers

Angle signals were not acquired in this first procedure, nevertheless before acquiring signals on muscles of knee, the electrogoniometers were placed (but not connected) on the right leg (lateral side) following the Biometrics guideline: they have to be positioned with spring in fully elongation along anatomical axes of the segment of interest. Subjects were set on a physiotherapy table for the second part of the first experiment and also for the second. Therefore this choice made easier the setup avoiding the patient to stand and sit after positioning all grids and cables. Subjects were asked to keep anatomical neutral position to find anatomical landmarks: greater trochanter, upper tibia and malleolus. Two segments were drawn on subject skin, the first between greater trochanter and upper tibia, the second between upper tibia and malleolus. As shown in figure 3.10 knee and ankle electrogoniometers were arranged along these two segments, respectively. Double-sided tape foam and hypafix have been used to avoid detachment of the electrogoniometers during the movements.



FIGURE 3.10: *Knee first experimental procedure: electrogoniometers placement for ankle and knee joint.*

3.4 Second experimental procedure setup

In this part of the experiment emg signals and angle signals were acquired from muscles of the two joints of interest, for this reason electrodes grids of muscles of the ankle and electrogoniometers were connected to the acquisition system. In the second procedure there is no contact between foot and floor. This is in contrast to the first procedure where tiptoe and heel were in full contact with floor during plantarflexion and dorsiflexion of the ankle, respectively. This could entail a different motion range of the ankle in the first and in the second procedure, mainly about plantarflexion. Hence an elastic bend has been assembled and its length has been adjusted depending on the leg of the subject. It had twofold purpose: the first was to force about 90 degree position between sole of the foot and the leg, the second was to generate a resistant force to plantarflexion (see figure 3.11).

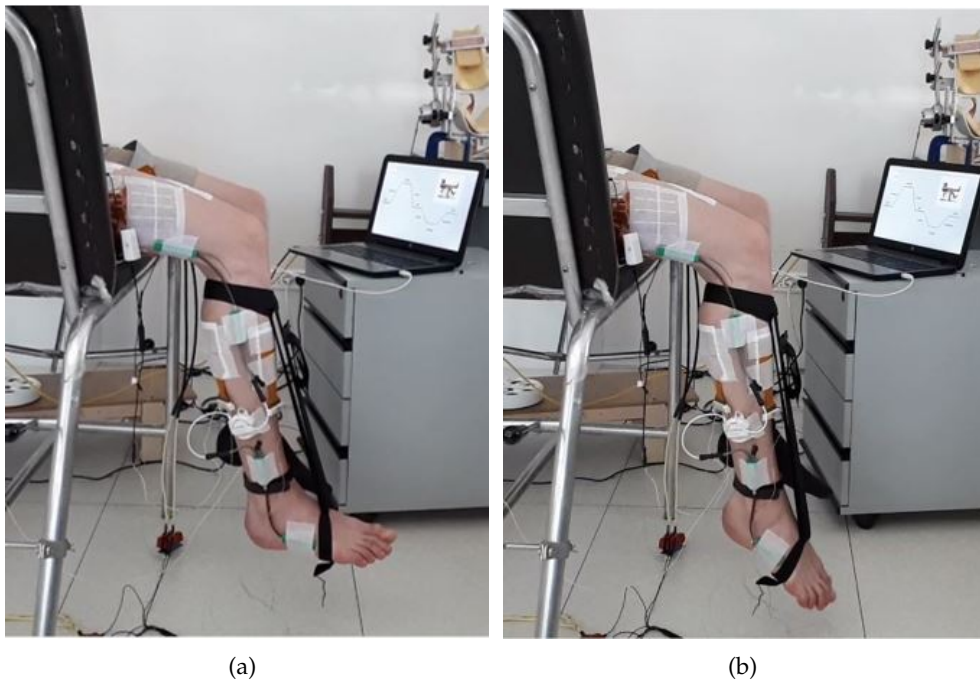


FIGURE 3.11: *Second experimental procedure: (a) both joints are in rest position and (b) knee is the rest position and ankle performed plantarflexion.*

3.5 Data analysis

3.5.1 Preprocessing

Monopolar emg recorded were bandpass filtered using a 4th order Butterworth filter between 20 Hz and 400 Hz. Powerline interference was removed by 50 Hz recursive filter. Since monopolar configuration has a higher signal-to-noise ratio (SNR) than bipolar configuration [7], bipolar emg were derived along longitudinal axis of the muscle. Hereafter bad channels were located and removed from further analysis using a graphical user interface realized in MATLAB[®]. Bad channels found in each movement were put together, then a complete list was removed from every movement. This to ensure that number of electrodes was the same for all trials performed.

3.5.2 Feature extraction

In this study logarithm of emg signal variance (log-var) were extracted from all available bipolar channels on non overlapping epochs of 250 ms [3]. Consequently, trajectory cues of first experiment and angle signals recorded in second experiment were downsampled to 4 Hz. The choice of this feature depends on the use of linear regression model, indeed to obtain reasonable performance with this model the relationship between emg feature and motion data should be as linear as possible. It has been confirmed in several studies [5], [6] that log-var feature shows best linear characteristic with respect to joint angles. At the end of these operation a feature matrix was obtained, whose columns were feature samples, and rows were the number of bipolar electrodes available.

3.5.3 Regression model

Regressor predicts a continuous target variable from a continuous input features. To fit the underlying problem it is important to choose a suitable complexity for the regression model, because a too low complexity of the model not allows to approximate target variables adequately, and a too high complexity increases the risk of overfitting to the training data. Complexity should be high enough to model the underlying problem, for this reason regularization techniques can be used.

Let $\mathbf{X} \in \mathbf{R}^{C \times S}$ denote the feature matrix whose columns correspond to C dimensional feature vectors that is the number of bipolar channels of a single joint for the s-th time observation $x_s = (x_s^1, \dots, x_s^C)^T$ and $\mathbf{Y} \in \mathbf{R}^{D \times S}$. \mathbf{D} is the number of DoF considered, particularly D is one in the first experimental procedure for ankle and knee, whereas D is two in the second experimental procedure where DoFs of ankle and knee were evaluated simultaneously. A linear regression model has the form:

$$\hat{Y} = W^T X + w_0 \quad (1)$$

where \hat{Y} is the angle signals approximation of Y . Since angles were not recorded in the first experiment, Y is the angle signal defined by user using angles values found in literature for ankle and knee joint (see section 3.1.1.1 and 3.1.1.2). $W \in \mathbf{R}^{C \times D}$ is the matrix of regression coefficients $w_d = (w_d^1, \dots, w_d^C)^T$. w_0 is the bias that has been included in W by extending all X_s with the constant 1. Minimize the sum of squared residuals of the linear regression model is the approach chosen to fit the linear model:

$$\hat{W} = \underset{W}{\operatorname{argmin}} \sum_d (y_d - w_d^T X)(y_d - w_d^T X)^T \quad (2)$$

However a ridge regression model is used, hence a regularization term including the L_2 norm of W in (2) has been added:

$$\hat{W}^{\text{ridge}} = \underset{W}{\operatorname{argmin}} \sum_d (y_d - w_d^T X)(y_d - w_d^T X)^T + \lambda_2 \sum_c \sum_d \|w_d^c\|_2 \quad (3)$$

the regularization parameter that controls the amount of shrinkage of the coefficients is $\lambda_2 \geq 0$: as λ_2 is increased, the coefficients are shrunk toward zero. The solution of the ridge regression optimization problem can be obtained in a closed form:

$$W = (XX^T + \lambda_2 I)^{-1} XY^T \quad (4)$$

where I is the identity matrix. Optimization of λ_2 parameter is developed by a grid search with a nested cross validation [5].

3.5.4 Nested cross validation

A ten-fold nested cross-validation was applied to evaluate the performances of reconstructing trajectory angles. Data set was made of 10 movements and it was split into 10 folds: one movement in each fold, therefore leave-one-out cross-validation has been performed. Lasso works at the outer level of the nested cross-validation selecting emg channels then ridge regression model calculates weights for these subsets in the inner level. In details nine folds were used as training data for selecting channel subsets, several configurations for every subset were found. In the inner part the best configuration was identified evaluating the performances of weights associated to that particular configuration. From nine folds used in the outer level, eight were used as training data and one as test set for calculating weights in the inner part. To this end, optimization of λ_2 parameter was performed. The optimal parameter value λ_2 in equation (4) has been

determined through a grid search strategy [5]. This procedure was repeated until all ten folds were tested once. The data set remaining in the outer part was used to identify the best one, evaluating the performances of the linear model. Since ten fold cross validation was applied, ten are the possible configurations of weights for a specific subset. Note that the movements used as training set or test set were provided randomly concatenated to Lasso and regressor. As a performance metric r^2 was used:

$$r^2 = 1 - \frac{\sum_i (y_i - f_i)^2}{\sum_i (y_i - \bar{y})^2} \quad (5)$$

where y_i and f_i are the angles defined by user for the single DoF and angles estimated by ridge regression method, respectively. The numerator is the residual sum of squares and the denominator is the total sum of squared.

3.6 Channel selection

The number of channels to select for the joint of knee and ankle was 196, 128, 96, 64, 32, 16, 8, 4 and 84, 64, 48, 32, 16, 8, 4, 3, respectively. The number of electrodes in every subset has been chosen thinking about the setup realized in the first part for ankle and knee joint. As described in the previous section, 10 fold nested cross validation was applied to select subsets using Lasso, construct their linear regression models by ridge regression method, and evaluate the performance of decoding angles using r^2 . This procedure was applied for the joint of knee and ankle separately

3.6.1 Lasso

Lasso [15] is shrinkage method that differs from ridge regression because it provides a sparse solution by using L_1 penalty insted of L_2 ridge [8]; the model is given as:

$$\hat{W}^{Lasso} = \underset{d}{\operatorname{argmin}} \sum_d (y_d - w_d^T X)(y_d - w_d^T X)^T + \lambda_1 \sum_c \sum_d \|w_d^c\|_1 \quad (6)$$

where $\lambda_1 \geq 0$ is regularization parameter that controls the amount of sparsity of coefficients. The larger values of λ_1 are, the smaller number of non zero regression coefficients is led. This provides an effective subset selection method [15]. For this reason optimization process of this parameter has been carrying out by empirical procedure. Therefore channel selection can be performed eliminating channels that correspond to zero coefficients. Lasso coefficients are shrunk toward zero in order to find sparse solutions, as a result Lasso coefficients are generally biased [2]. For this reason the purpose of Lasso is only to select channel subsets: zero coefficients correspond to not informative channels, therefore these channels are discarded, whereas non zero coefficients are considered informative channels and hence selected. Ridge regression method has been used to find and optimize weights only for the channels found by using Lasso [2]. Lasso function implemented in MATLAB[®] has been used to perform channels selection. If any values of λ_1 is supplied, this function calculates only the larger values of λ_1 that not gives a nonnull model, then the ratio between smallest to the largest value of this sequence and the length of the vector of λ_1 values. Experimentally has been noticed that this vector, automatically chosen, is not sufficient to ensure the selection of any number of feature (this case related to emg bipolar channels). For this reason a vector of λ_1 values has been defined by user and provided to this function. The vector contains a large number of values logarithmically spaced. Moreover, algorithm was implemented in order to accept only solutions containing exactly the number of channels required.

3.7 Training data reduction

For clinical applications the training time should be as short as possible to reduce the time to fit exoskeleton. To this end, the proposed method was evaluated varying number of data used as training and test set. On the whole four cross validation were implemented:

1. leave-one-out cross-validation, data set is complete (10 movements);
2. leave-one-out cross validation, data set was reduced by 50%;
3. train set = 40% of data set complete, test set = 60% of data set complete;
4. train set = 40% of data set reduced by 50%, test set = 60% of data set reduce by 50%.

3.8 Robustness test

To investigate the robustness of the channel selection reducing training data, three tests has been developed considering also the main procedure described in the section 3.5.4.

3.8.1 IED evaluation

Since a k-fold cross-validation is performed to select every subset, there are k possible configurations for a specific subset. The way to identify the best one is described in 3.5.4. Channels selected in all these configurations for the i-sh subset are defined in common. There is a need to locate the channels not in common, because in many cases one electrode is in all configurations except one. This is a way to verify if not in common channels of different configurations of the same subset are close to each other. For this reason, IED was calculated among channels not in common belonging different configurations for the same subset. This evaluation has been performed on each single muscle.

3.8.2 Subsets weight homogeneity

The best weight matrix of every subset was obtained in the inner part of cross validation through an average process of all matrix weight corresponding to the optimal value of λ_2 found. Thus, the variation of the weights associated to same channels for every subset has been examined.

3.8.3 Overlap ratio

To investigate the feasibility of reducing data training, the overlap coefficient [16] has been calculated to measure for every subset the similarity between the electrodes selected operating the four different data reduction and to verify how many channels are in common between each subset and its previous:

$$\text{overlap}(X, Y) = \frac{|X \cap Y|}{\min(|X|, |Y|)} \quad (7)$$

where X and Y are the two sets took in exam. The coefficient is calculated dividing the size of the intersection by the smaller size of the two sets. If one of the two set is a subset of the other, the overlap coefficient value is 1.

3.9 Angles decoding

In the second experiment, to reconstruct angles signals linear regression model has been used as in section 3.5.3, indeed the model is the same described in (1) but with some differences: $\mathbf{X} \in \mathbf{R}^{C \times S}$ is the feature matrix where C is the number of all available bipolar channels calculated for ankle (84) and knee (196) for the s -th time observation. X is made of concatenating ankle feature matrix with knee feature matrix along columns. \hat{Y} denote the angles estimation of $\mathbf{Y} \in \mathbf{R}^{D \times S}$, D is two because we are evaluating two DoFs simultaneously. Despite the first experiment, in the second angles signals from both joints have been recorded by electrogoniometers. $\mathbf{W} \in \mathbf{R}^{C \times D}$ is the matrix of regression coefficients of both joint, the first and the second column contains matrix weight of the ankle and knee respectively. Since eight subsets were defined for each joint (see table 3.1), complete matrix of weights obtained were eight. A complete matrix of weights has the form:

$$W = \begin{bmatrix} w_1 & 0 \\ \vdots & \vdots \\ w_{84} & 0 \\ 0 & w_{85} \\ \vdots & \vdots \\ 0 & w_{280} \end{bmatrix} \quad (8)$$

Emg acquired in second experiment followed the preprocessing described in section 3.5.1 and 3.5.2 except for bad channels. To avoid mismatch of dimension between W and X , bad channels eliminated in the first experiment were supposed to be the same also in this second experiment, thus they were reinserted in W but their weights were force to be zero.

Channel subsets								
Ankle	196	128	96	64	32	16	8	4
Knee	84	64	48	32	16	8	4	3

TABLE 3.1: Channel subsets defined for ankle and knee joint.

Chapter 4

Results

4.1 First experiment results

4.1.1 Impact of reduced training data

Figure 4.1 shows the mean r^2 value of all channel subsets found in each cross validation implemented. A comparison between results obtained from subjects 1 and 3 has been done.

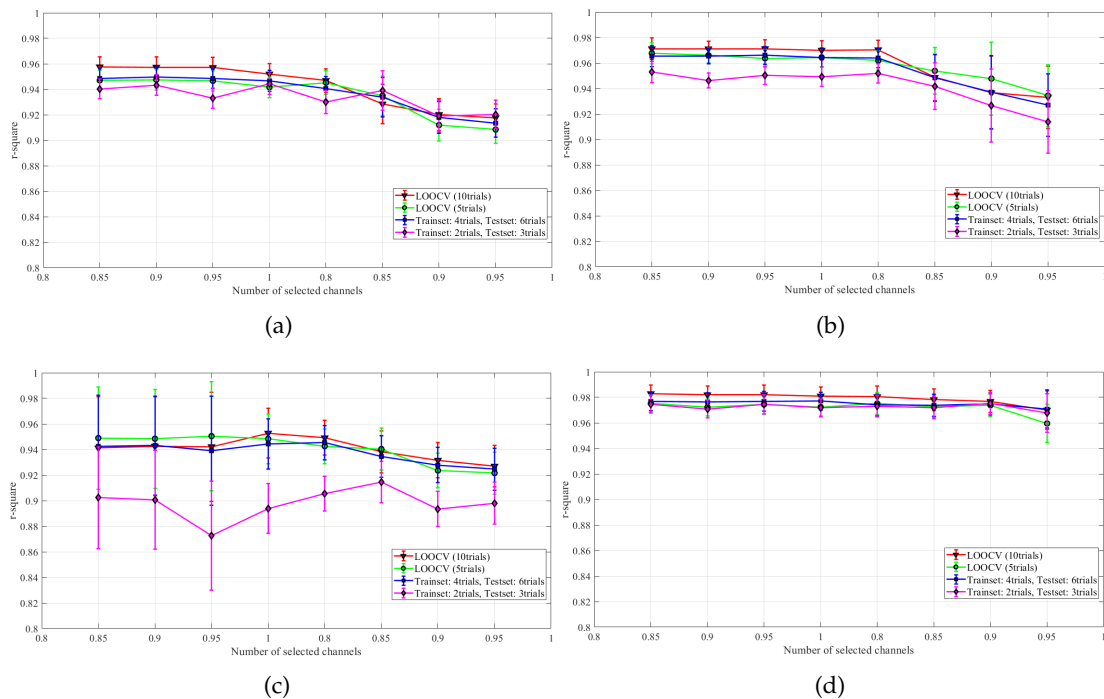
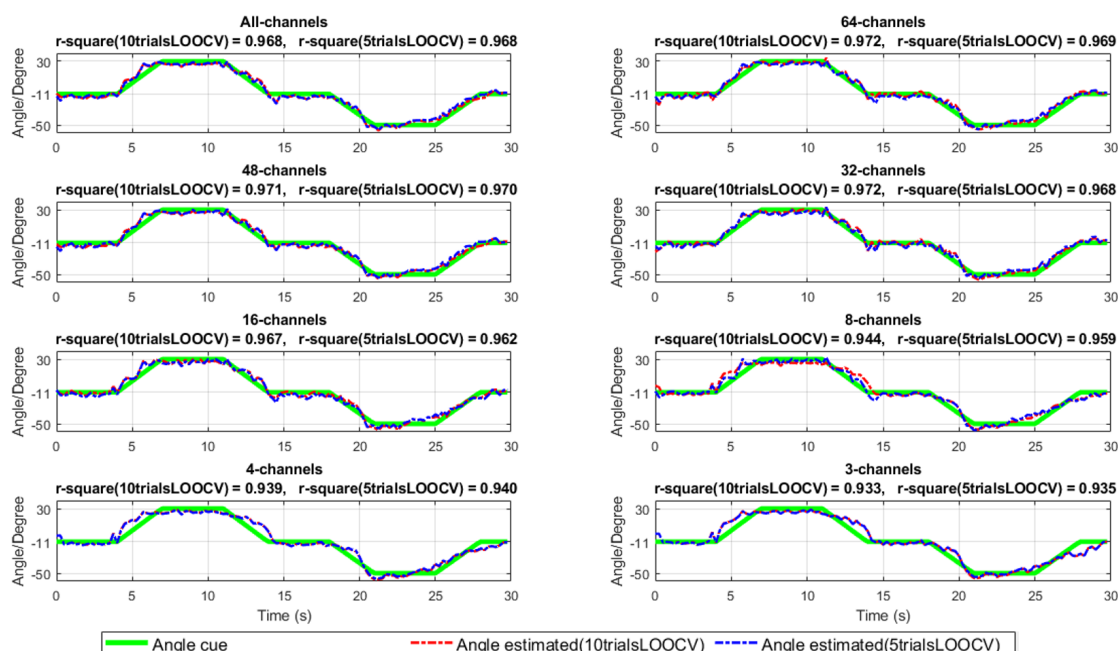
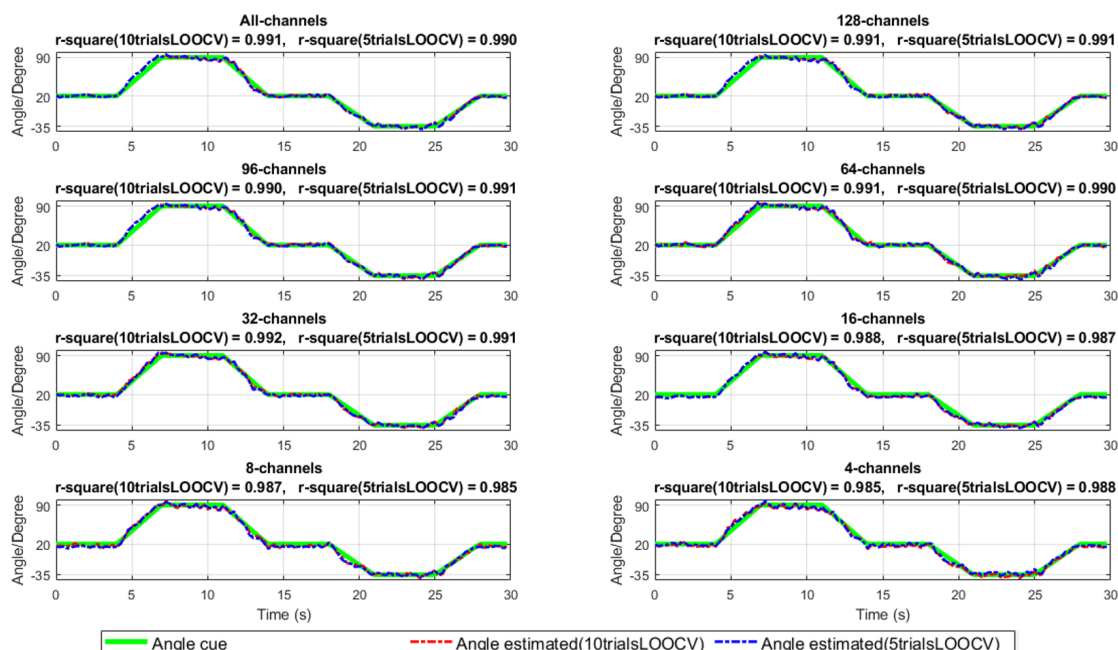


FIGURE 4.1: Performances of all subsets of channels selected for (a) ankle and (b) knee joint of subject 1 and for (c) ankle (d) knee joint of subject 3. The vertical bars represent the standard deviation of the r^2 estimated for every channel subsets.

It can be seen as the number of electrodes is reduced the performances had the same trend for both joints: they were constant for the first four subsets and then they decreased considerably when electrodes were reduced by 60% and 80% for ankle and knee, respectively. This occurs regardless of the number of movements used in the train and test set, even if the lowest trend is obtained when only two trials were used to train (purple line in figure 4.1(c)). In the first experiment, but also in second, performances of channel subsets found for knee are generally higher than those found for ankle. Moreover, from these figures appears that performances obtained with 10 trials LOOCV and 5 trials LOOCV are comparable in almost all subset configurations, this behavior is the same in all subjects. For this reason, results from only these two types of cross validation will be analyzed in the following sections. An intuitive example of the performances estimated above is provided in figure 4.2 (a) for the ankle and in figure 4.2 (b) for knee. The best channels configuration for each subset is used to estimate angle signals of two joints separately. Note that in the first experiment angles for both joints were not recorded but provided by a target trajectory on a screen, indeed the regressor output (the trapezoidal cue) is the same for all 10 movements of the subject. The green line in 4.2 represents the trajectory followed by subjects, and the dashed lines coloured in red and blue represent the estimated angles using 10 trials LOOCV and 5 trials LOOCV, respectively. In each graph blue line superimposes the red one, there is evidence that high accuracy performances were achieved either using 10 trial LOOCV or 5 trials LOOCV. It means that for this first part of the protocol, 5 trial are enough to obtain satisfying performances in angles decoding. In each graphic, r^2 values displayed for both methods are comparable high, but whereas the angles decoded for knee are very close to trapezoidal cue, angles for the ankle shows some inaccuracies when number of electrodes is drastically reduced. Especially during dorsiflexion (see 4.2 (a) between about second 5 and 15) and plantarflexion (see 4.2 (a) between about second 18 and 28). It is hard to follow the green cue in the ascending and descending phase, this can be seen particularly in configuration of 3-channels or 4-channels. Moreover, once subjects got the maximum range of plantarflexion (between 20 and 25 second), probably they decreased the contraction instead keeping it constant for the duration of this hold phase. This can be seen in 3-channels configuration where blue and red line start to rise before second 25.



(a)



(b)

FIGURE 4.2: An example of (a) ankle and (b) knee angles reconstruction respect to the number of selected channels. Green line is the trajectory target, the red and blue dashed line represent angles estimated related to 10 trials LOOCV and 5 trials LOOCV. Data derived from trial 8 performed by subject 3.

4.1.2 Robustness test

4.1.2.1 Consistency of electrode selection

In this analysis minimum distance between channels not in common among different configurations of the same subset was evaluated. As shown in figure 4.1, mean r^2 values are high and the confidence interval are small, this figures out that for both joints almost all possible configurations for a specific subset are similar but they differ by some electrodes. Figure 4.3 gives information about the percentage of channels in common among different configuration of the same subset averaged on all subsets, this has been evaluated for each four different cross validation methods. The behavior is the same for both joints: the more trials are used the higher the percentage of channels in common among configurations of same subset is. Moreover 4.3 (a) shows a little difference between 10 trial LOOCV and 5 trial LOOCV whereas for the knee, in 4.3 (b), this difference is significant, probably this is due to the greater number of electrodes used for knee than ankle.

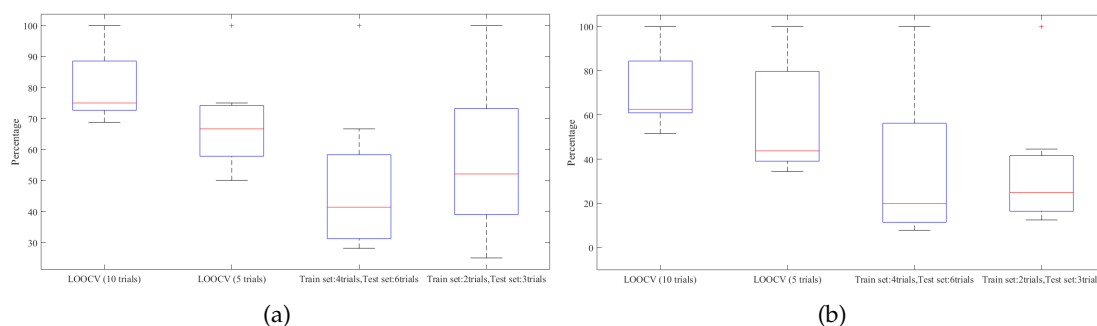
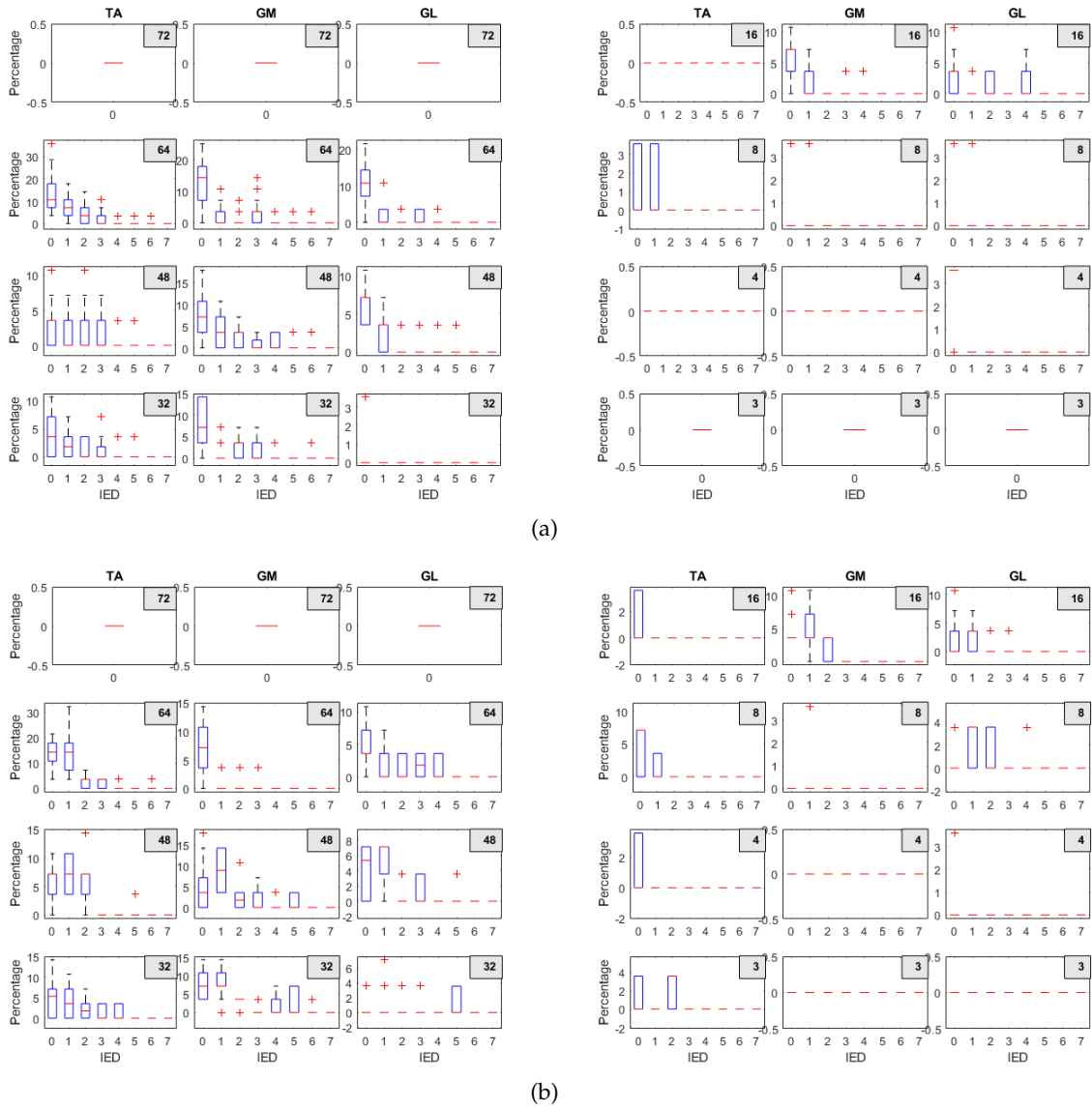


FIGURE 4.3: *Percentage of channels in common among different configurations of same subset averaged on all subsets of a specific cross validation method. Data displayed are related to analysis on (a) ankle and (b) knee joint of subject 3.*

In order to verify if electrodes not in common among configurations of same subset were however located in the same area, IED evaluation has been performed on every muscle separately. Results related to the muscles of the ankle and knee are displayed in Figure 4.4 and 4.5, respectively. The x-axis shows the interelectrode distance available for a specific muscle, namely for a specific electrodes grids. Note that the electrodes grids used were made of 32 and 64 electrodes, but as described in section 3.5.1 bipolar signals have been used. For this reason, considering bipolar emg signals, electrodes matrix consisted of 28 (7x4) and 56 (8x7) electrodes. Hence the maximum IED available for the two grids described before was 7 and 9, respectively. Gray labels were applied to better identify each subset of channels. On x-axis there is also IED equal zero, this because

experimentally has been noticed that some of these electrodes not in common belong to most of the configurations available for a subset except few of them. Therefore when all channels not in common of a subset were evaluated, if two configuration had same electrodes their IED in that case counted zero. In case of complete number of electrodes this evaluation has not been performed. For example, the graphics related to tibialis anterior with subset of 64-channels, in the upper part of figure 4.4 (a), shows that about 25% of all electrodes of this muscle are electrodes not in common between different configurations for this subset of 64-channels. In details slightly above 10% of these electrodes not in common has IED equal 0, less than 10% has IED equal 1 and 2. As the number of trials is reduced, minimum IED between electrodes not in common is increased slightly, an intuitive example is provided by values related to tibialis anterior (96-channels subset) and vastus lateralis (128-channels subset) shown in figure 4.4 (b) and 4.5 (b), respectively. Nevertheless, this phenomenon seems affects quantitatively more higher channel subsets than the lower, particularly first four subsets of each joint. This can be appreciated comparing results from 10 trials LOOCV and 5 trials LOOCV reported for ankle and knee joint in figure 4.4 and 4.5 respectively. Moreover, what displayed in these figures occurs for every subject of this study: the majority of electrodes not in common for ankle muscles are related to a IED range between 0 and 2, whereas in the case of knee this range is wider: from IED equal 0 up to IED equal 3. Probably it occurs because of larger dimension of the electrodes grids placed on muscles of knee. Regardless this difference between joints, both methods have proved to be suitable providing robust results: IED between electrodes not in common for a specific subset is contained, it means that also these electrodes are chosen near the same muscular region of interest.



(a)

(b)

FIGURE 4.4: (a) 10 trials LOOCV and (b) 5 trials LOOCV data for the evaluation of distance between channels not in common among all available configurations for every subset. The analysis was performed on each muscle of ankle separately. Data were derived from subject 3.

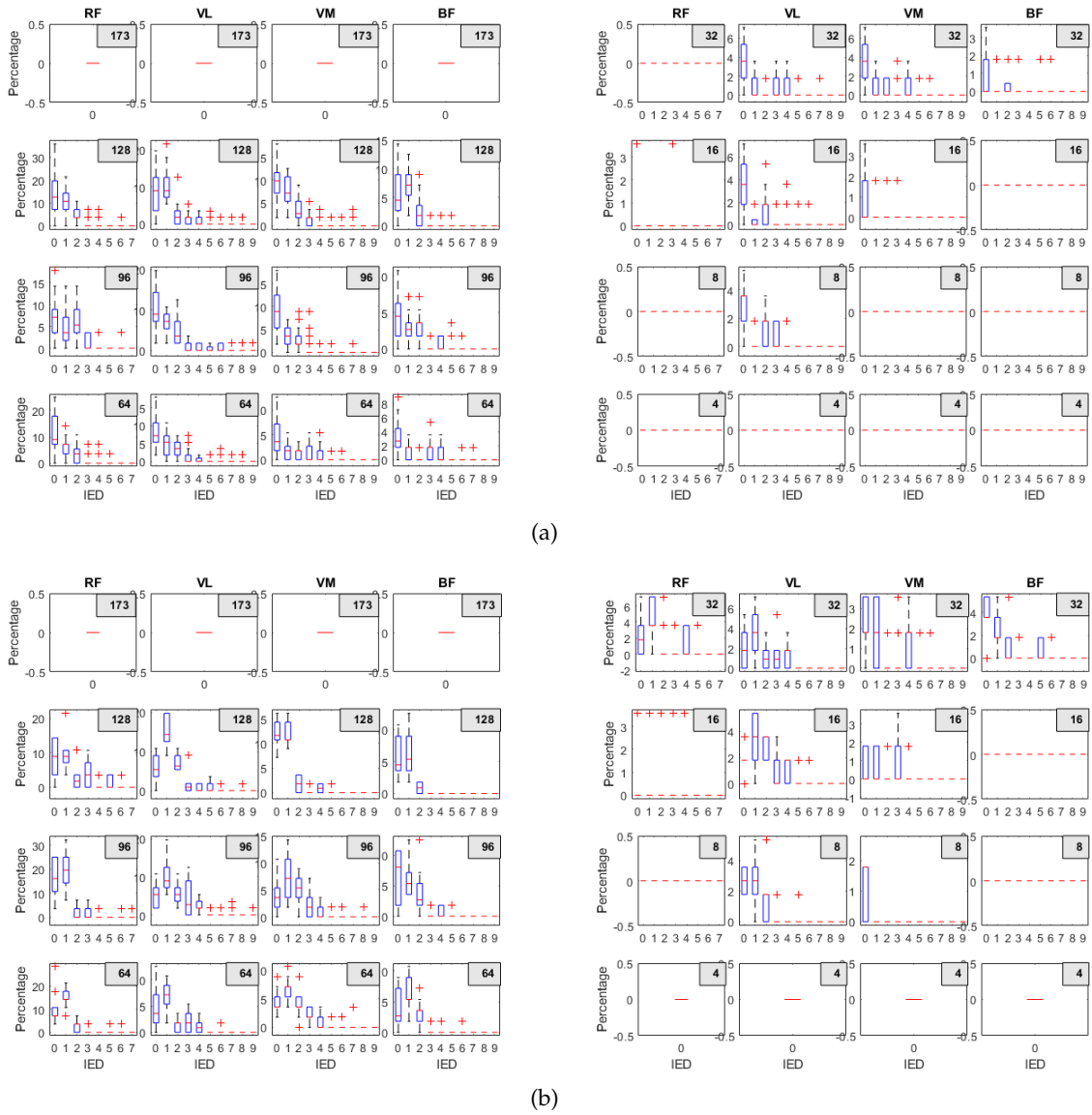


FIGURE 4.5: (a) 10 trials LOOCV and (b) 5 trials LOOCV data for the evaluation of distance between channels not in common among all available configurations for every subset. The analysis was performed on each muscle of knee separately. Data were derived from subject 3.

4.1.2.2 Subsets weight homogeneity

In the previous sections, channels of different configurations available for the same subset were analyzed. Indeed, it has been proved that all possible configurations of channels selected for a specific subset have the majority of electrodes in common, and also those not in common are localized rather close to each other. But same channels in more configurations means not necessarily same weights associated to them. This because as explained in section 3.5.4, lasso selected channels and then regression was used to estimate their weights. For example in 10 trials LOOCV method, each best channels configuration of each subset has 9 possible configurations of weights. One of these weight configurations is the best for the subset selected by lasso. To verify the robustness of this approach, variation of all weight configurations associated to best channel selection for every subset has been examined. Figure 4.6 (a) shows result for ankle and Figure 4.6 (b) for knee. Moreover, for each joint an additional comparison between different cross validation methods has been done.

All possible weights for each channel of a subset have been normalized to the maximum weight found, this value has been chosen as reference in order to obtain a distribution of percentage between 0% and 100%. The median gives overall information on how weights variate their values with respect the normalization value. But regardless these values, upper and lower interquartile gives the most meaningful information. Indeed, it can be appreciated that variation of weights are generally around 30% in first 5 subsets of each joints, regardless of the method. On the other hand, it can be seen that wider variations are achieved for last three subset of each joint, probably due to the limited number of channels. It is interesting to note that, number of trials used to obtain data seems not affect particularly variation of weights, indeed comparing subsets of different methods figures out that distance of lower and upper interquartile are almost the same in each method, except in case of lower number of electrodes.

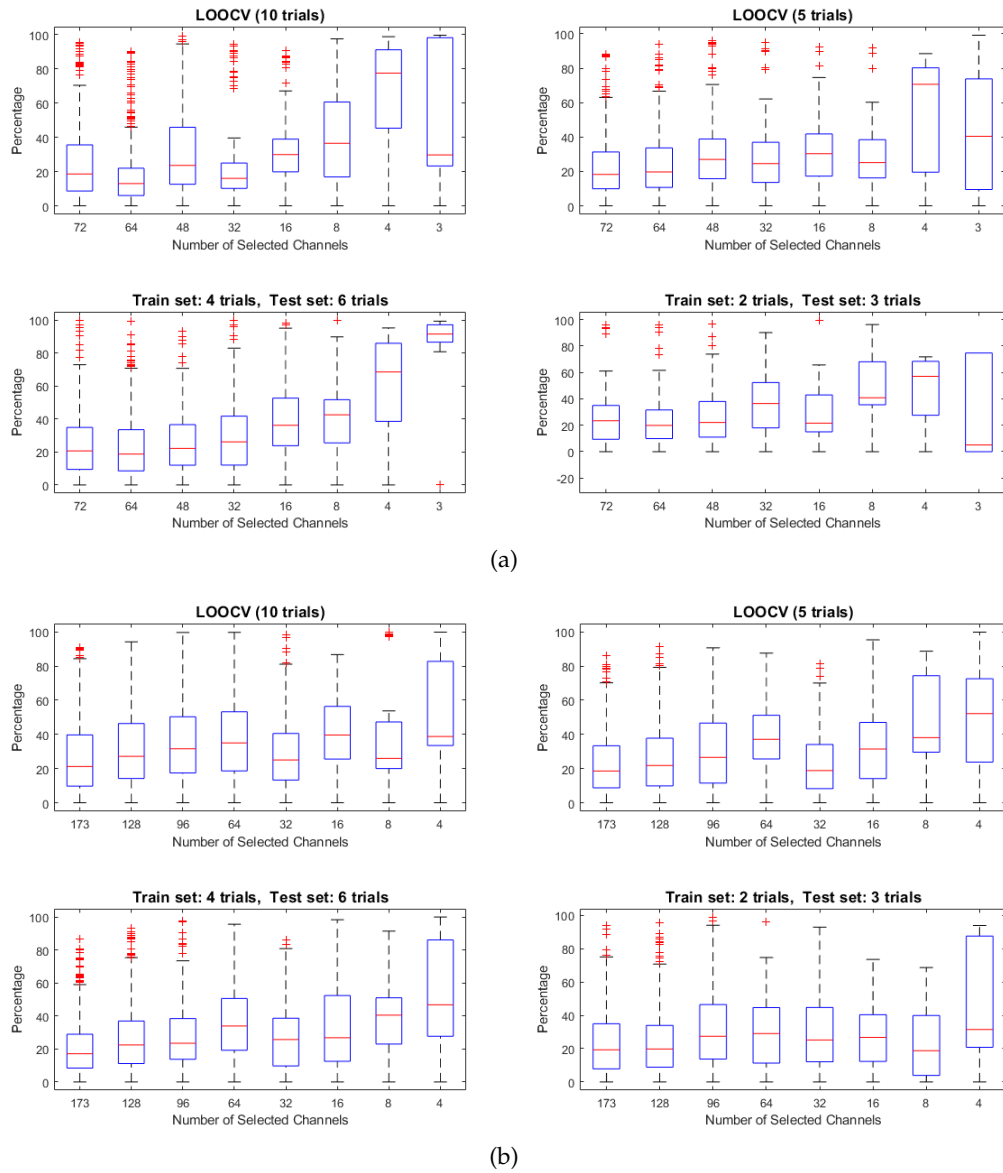


FIGURE 4.6: Graphics show weights variation of all available weights associated to channels of best configuration selected for each subset. (a) Ankle and (b) knee data were taken from subject 3 analysis. To evaluate how number of trials affected weights variation, this analysis has been conducted for the four different cross validation.

4.1.2.3 Overlap ratio

Overlap ratio illustrated in figure 4.7 (a) for ankle and 4.7 (b) for knee, shows intersection of best channels configurations found for each subset using the 4 different cross validation methods. It is interesting to see that overlap ratio decreases significantly as the number of electrodes is decreased across 4 methods. Instead, 4.7 (c) and (d) display intersection of best channels configurations found for each subset between only 2 cross validation method: 10 trials LOOCV and 5 trials LOOCV. From these graphics it figures out that the trials reduction impacts in a significant way the performances of selection regardless number of channels for each subset.

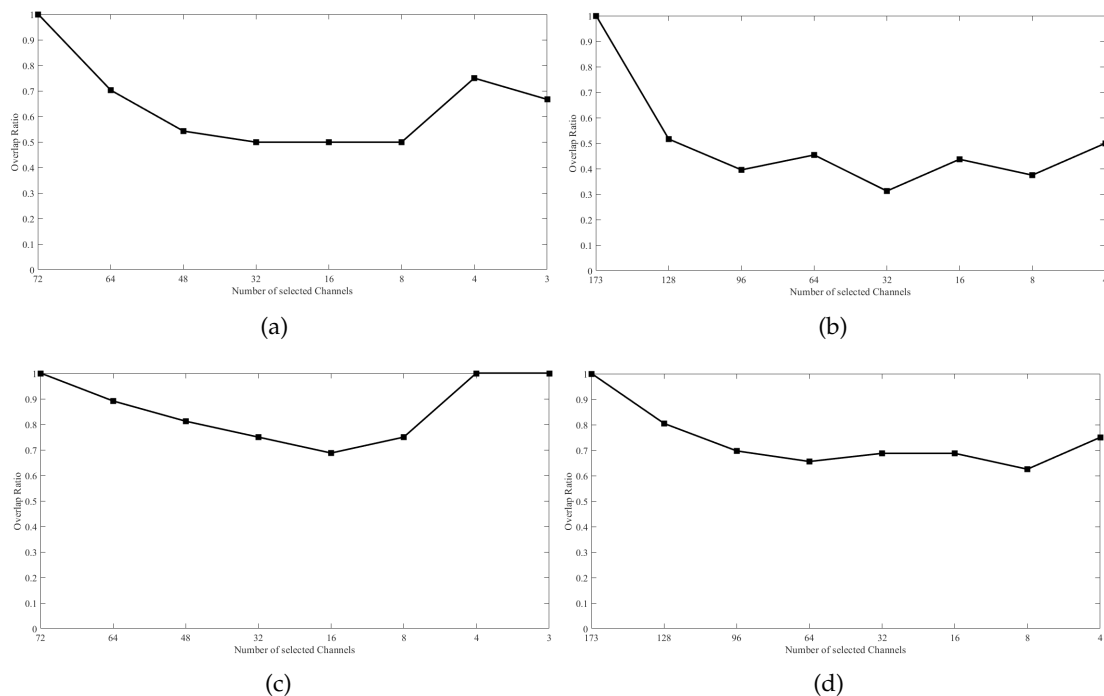


FIGURE 4.7: (a), (b) Overlap ratio of best channel configurations for each subset among 4 different types of cross validation. (c), (d) Overlap ratio of best channel configurations for each subset between 10 trials LOOCV and 5 trials LOOCV. (a), (c) Ankle and (b), (d) knee data derived from subject 3.

As touched upon, main methods took into account were 10 trials LOOCV and 5 trials LOOCV, hence overlap ratio has been calculated for these methods. In details, the intersection between each subset and its previous subsets has been evaluated. This analysis has the purpose to verify if there are some electrodes that contribute in all subsets, or almost all. Figure 4.8 and 4.9 provide an intuitive illustration of the results. In these figures, graphics related to the subset with the maximum number of electrode are empty

because this is the complete configuration. Title of single graphic indicate the current subset and on x-axis there are the previous subsets, on y-axis there is overlap ratio values explained between 0 and 1. For example, it can be seen that in figure 4.8 (a), particularly about subset made of 3-channels, all 3 electrodes chosen by algorithm were also chosen in all previous subsets, except for subset with 16-electrodes where only some of them were selected. About ankle results, overlap ratio has generally high performances, regardless of the number of trials halved in 5 trials LOOCV. For what concern knee, performances are lower in more subsets with few electrodes, moreover when trials were halved. As shown in figure 4.9 (b) overlap ratio in lower subsets is higher than in 8 or 4-channels subset of 4.9 (a) where trials are 10. Probably less number of trials provides a more precise channels selection. Unfortunately, performances related to 5 trials LOOCV depends on the trials selected. As mentioned, in this study when there is a need to reduce number of original trials selecting some of them, the selection has been randomly performed. Overall, for both joints, high performances results has been obtained for this test, this proved the robustness of the selection method applied.

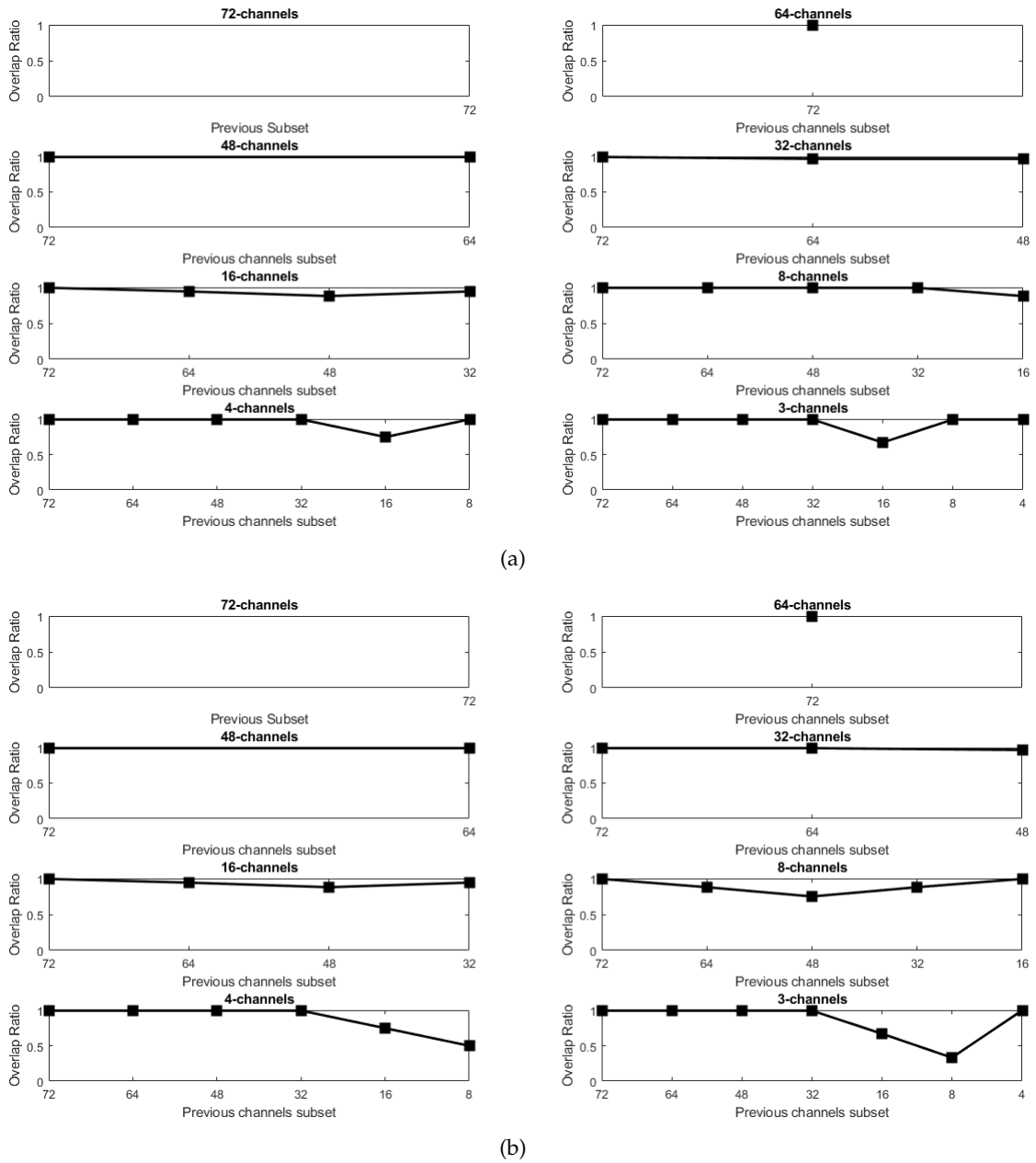


FIGURE 4.8: Ankle joint: overlap ratio used to evaluate intersection of best channel configurations between each subset and the previous. (a) 10 trials LOOCV and (b) 5 trials LOOCV data are derived from subject 3.

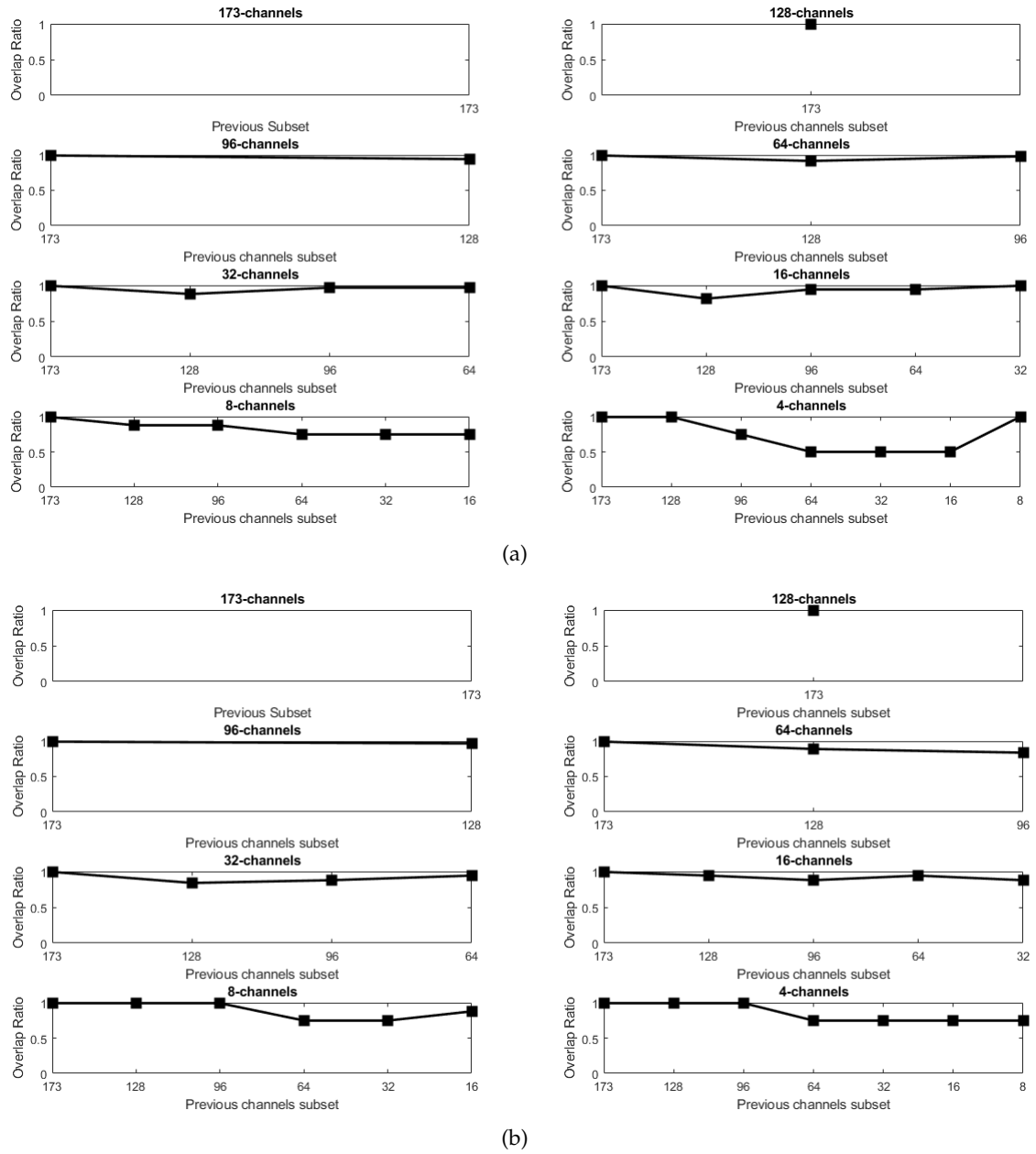


FIGURE 4.9: Knee joint: overlap ratio used to evaluate intersection of best channel configurations between each subset and the previous. (a) 10 trials LOOCV and (b) 5 trials LOOCV data are derived from subject 3.

4.1.3 Channel configurations obtained by Lasso

Figure 4.10 and figure 4.11 show an example of channel configurations of each DoFs (ankle and knee respectively) selected by Lasso and their coefficient weights related to a specific subsets. Channels chosen by Lasso are identified with symbol '+', whereas '△' is used to identify bad channels. Each colormap is related to a single muscle of the joint studied, all colormaps of each subset are equipped with a colorbar which shows intensity range of weights. Colormaps have the same dimension of bipolar channels grids, 7x4 for tibialis anterior, gastrocnemius medialis, gastrocnemius lateralis and rectus femoris, and 7x8 for vastus lateralis, vastus medialis and biceps femoris. Hence each colored box in a colormap represents a bipolar channels and its weight during the tasks. Complete configurations of both joints show which part of every single muscle is more informative during all duration of the task. As discussed previously, weights can be positive or negative, therefore most informative areas of each muscle are characterized by weights with high positive or negative coefficients. This pattern seems to be coherent also in the subsets with a lower number of channels. Looking at first four subsets of each joints, can be seen that each muscle has channels with weights both positive and negative. But examining the other 4 subsets of each joint, as the number of electrodes is decreased weights on each muscle became almost only positive or negative. In details muscular activation is described as follow:

- *ankle joint*: tibialis anterior is responsible for dorsiflexion, instead gastrocnemius medialis and lateralis are responsible for plantarflexion;
- *knee joint*: rectus femoris, vastus lateralis and medialis are dedicated to extension, whereas biceps femoris to flexion.

In the last 4 subsets of each joint, positive weights are principally on tibialis anterior, vastus lateralis and medialis, and rectus femoris whereas negative weights are on gastrocnemius medialis lateralis and biceps femoris. This behavior is observed in every subjects of this study, except one that shows weights of different sign in the same muscle. Could be a case of cocontraction, but in this study this aspect was not examine in deep.

Emg signals and the weight associated to them were analyzed, 3-channels and 4-channels subset of ankle and knee joint were examine in details.

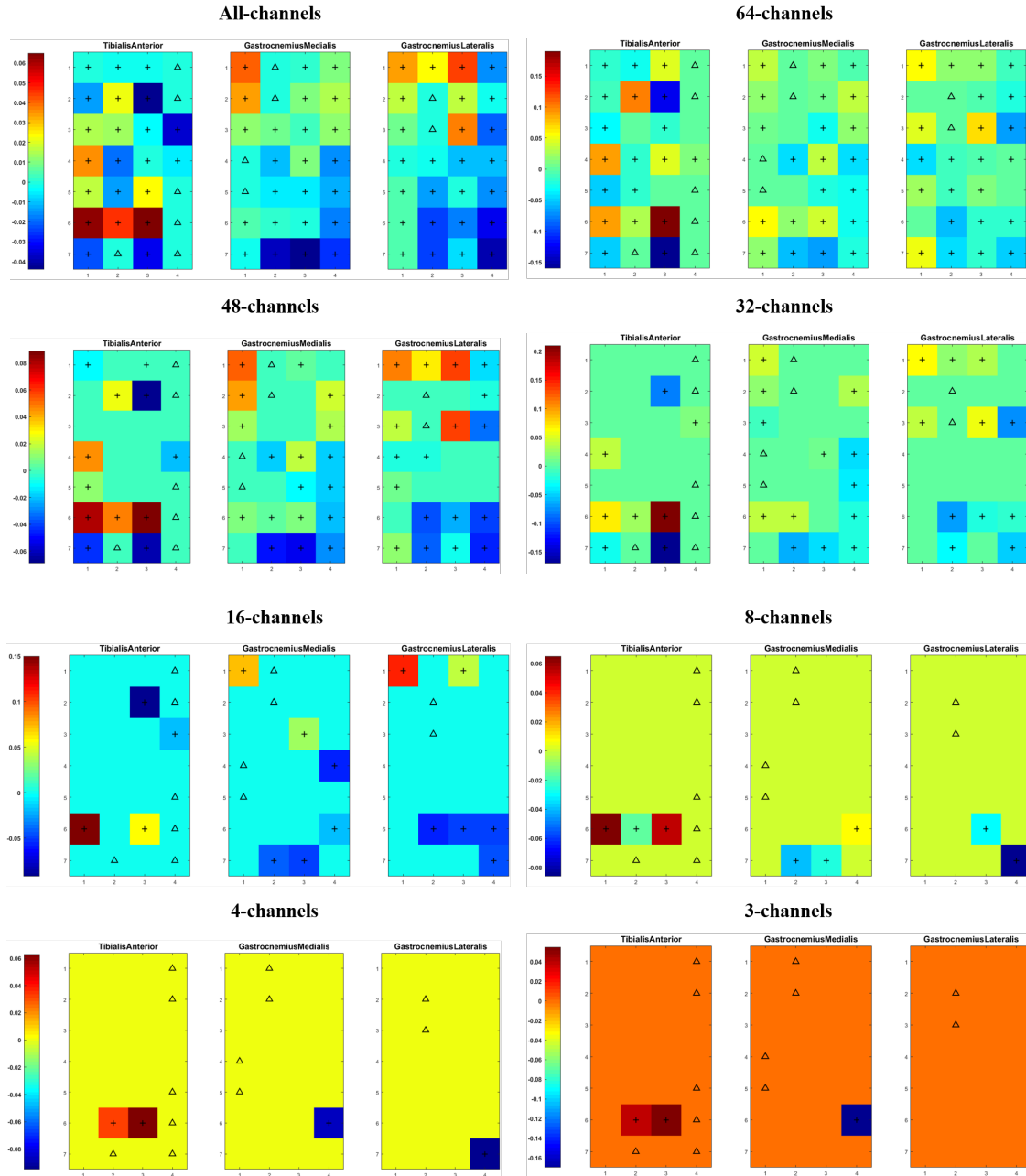


FIGURE 4.10: Colormaps show channels distribution and their coefficient strengths related to the number of channels selected for ankle joint. Matrix of regression coefficients used to illustrate coefficient weights derived from subject 3(10 trials LOOCV).

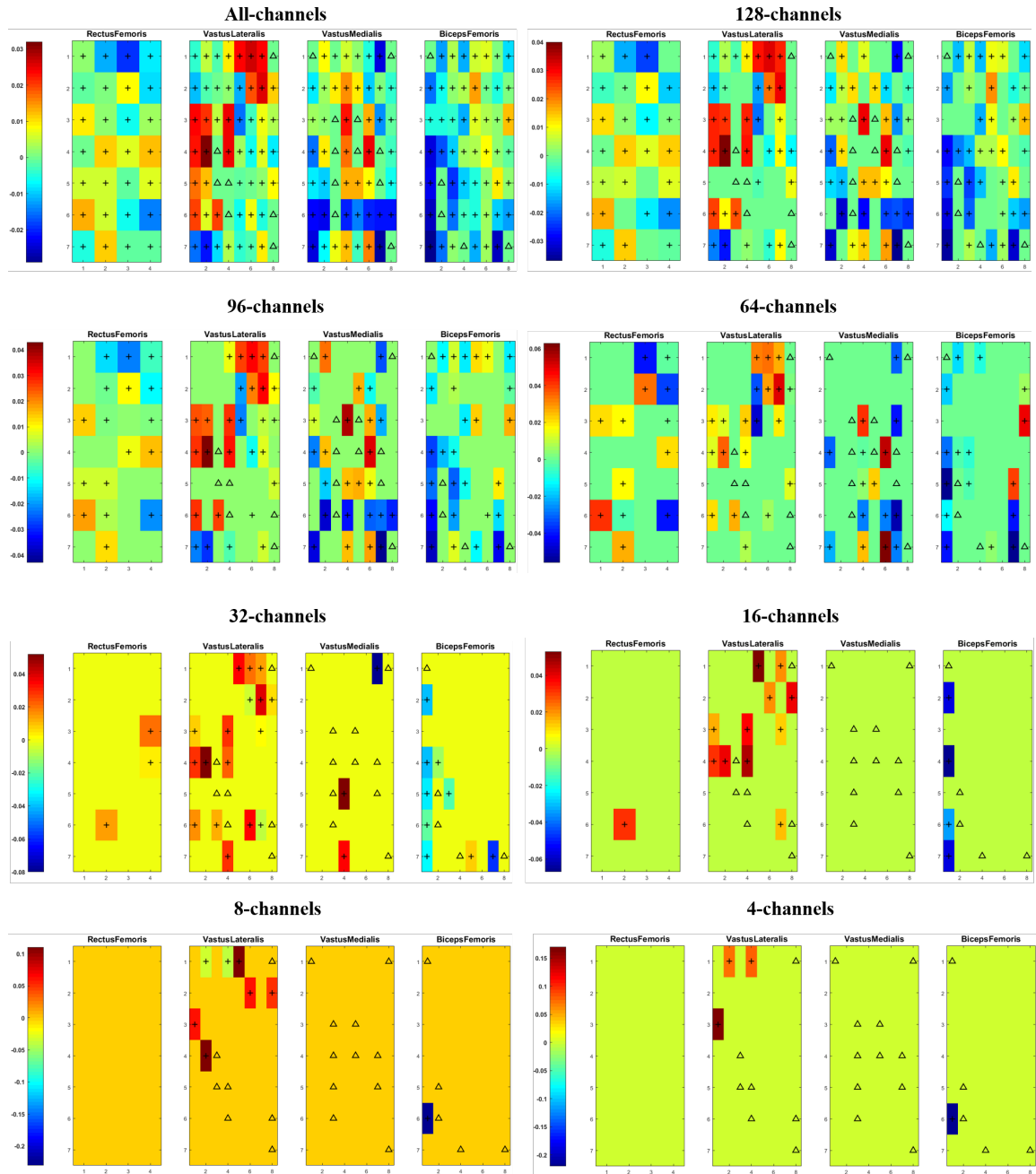


FIGURE 4.11: Colormaps show channels distribution and their coefficient strengths related to the number of channels selected for ankle joint. Observing x-axis of the colormaps, it is possible to recognize 7x4 grid (rectus femoris) and 7x8 grids (vastus lateralis, medialis and biceps femoris). Matrix of regression coefficients used to illustrate coefficient weights derived from subject 3 (10 trials LOOCV).

4.1.3.1 Ankle channel configuration analysis

As example, 3-channels configuration for the ankle is reported in figure 4.12 (b). Colormaps are oriented same way as electrodes grids are placed in figure 4.12 (a). It means that row 1, on y-axis, represents the most proximal part of the grid and consequently 7 represents the most distal portion. About x-axis, column 1 and 4 are the lateral and medial part of the grids. Note that in figure 4.12 (a) are displayed monopolar electrodes grids, whereas colormaps referred to bipolar signals. As discuss in advance, each coefficient weight is related to a bipolar channels, for this reason bipolar emg signals were provided in figure 4.13. In order to provide a better visualization, signals were normalized to the maximum value of each muscle grid, bad channels were discarded from this evaluation. Normalization value are shown in the title of 4.13 (a), (b), (c). On x-axis there is time line from the begin to end of the task, and on y-axis there are biological signals separated by offset. Red emg signals are the channels selected by Lasso corresponding to weights represented by '+' in the colormap. Bad channels identified in colormaps using the symbol ' Δ ' are displayed as horizontal null line. Graphics that include signals are made of as many columns as the column of the grids. Each column contains 7 bipolar emg signal, as 7 are the row of the grids of bipolar emg.

For what concern signals, examining tibialis anterior emg in figure 4.13 (a) it can be appreciated that each burst of activation is well defined in its proper activation interval between second 8 and 15. Activity was not recorded outside this activation interval, during which muscle is responsible for dorsiflexion. Quite different is the case of gastrocnemius medialis and lateralis, indeed figure 4.13 (b) and (c) show muscles activation between second 18 till the end, during plantarflexion, but it is possible to notice a lower coactivation in the same activation interval of tibialis anterior. This phenomenon is related not only to subject 3 but also to the others.

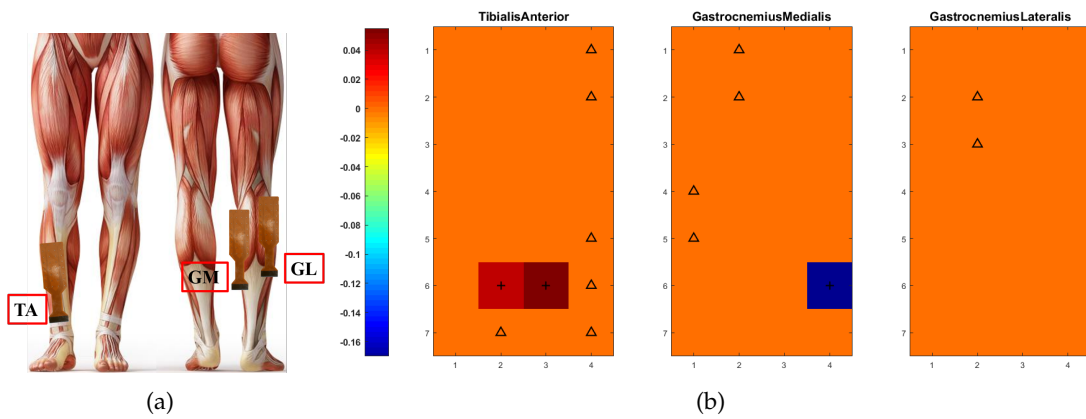
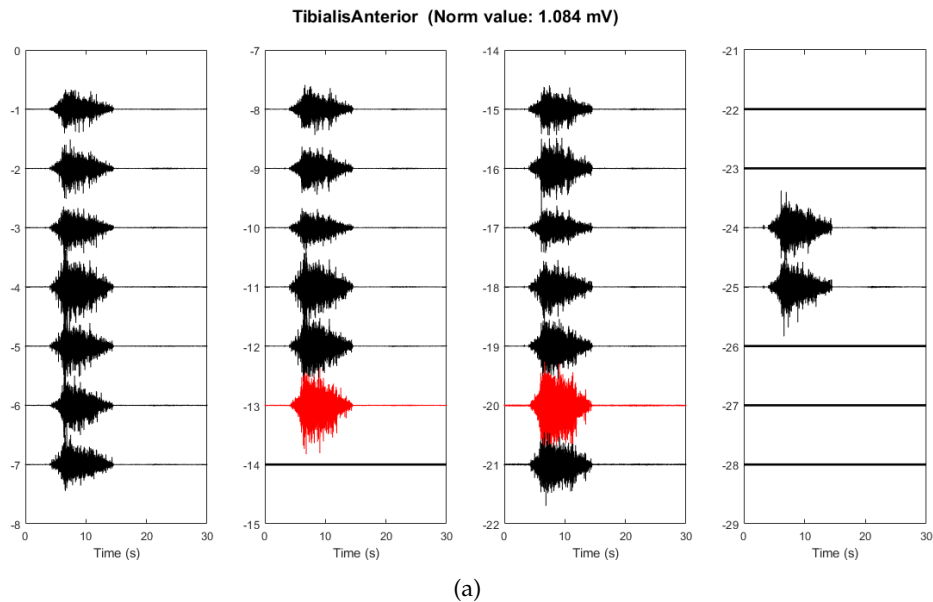


FIGURE 4.12: (b) Colormaps show channels selected for 3-channels configuration and their associated weights. Electrodes grids placement on ankle muscles has been reported in (a) to explain colormaps orientation. The order of channels displayed in the colormaps is the same as looking grids applied to the skin of the subject. Data are derived from subject 3.



(a)

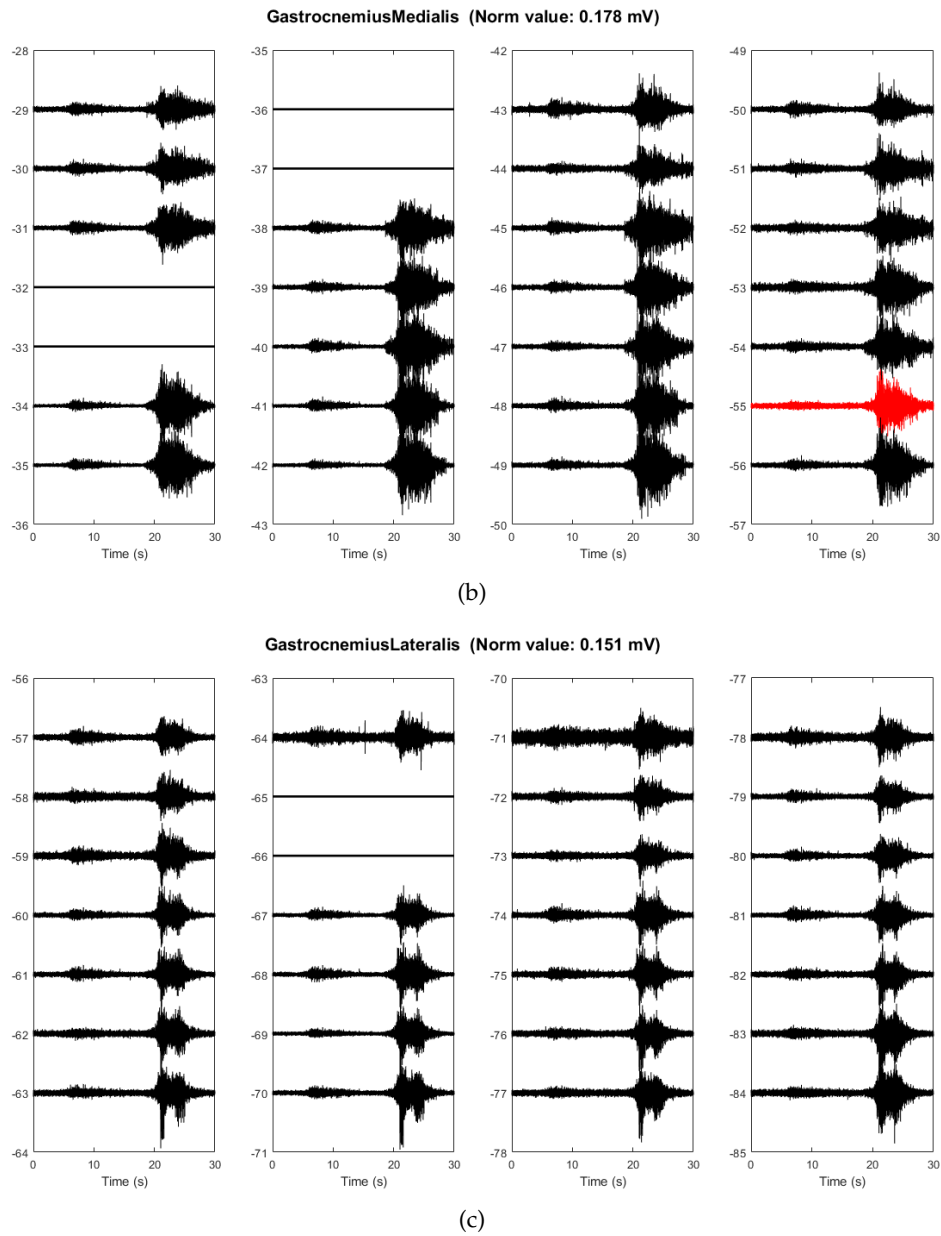


FIGURE 4.13: *Emg bipolar signals of (a) tibialis anterior, (b) gastrocnemius medialis and (c) gastrocnemius lateralis of subject 3 trial 4. Channels selected by Lasso are colored by red and bad channels were substituted by horizontal black line.*

4.1.3.2 Knee channel configuration analysis

4-channels configuration has been taken as example for knee joint. Observing figure 4.14 (b) it is possible to note that 4 channels selected by Lasso belong to vastus lateralis and biceps femoris, in details dark blue weight is related to semitendinosus due to its position in the grid. No electrodes has been chosen on rectus femoris and vastus lateralis. This choice recurs for the other four subjects configuration of 4-channels subset: no channels on rectus femoris, and only one presents one channel on vastus medialis. This means that probably there is a redundancy of information as far as concern vastus lateralis and medialis, whereas perhaps rectus femoris was discarded because of its low activity. Indeed, in figure 4.15 (a) it is possible to distinguish bursts of activation of rectus femoris from remaining trace of signal, but the activity level of the burst is not so different from the level of the complete trace. This could be done to thicker adipose tissue on this muscle, this could explain the attenuation of the activity recorded for this muscle. For what concern vastus lateralis seems that this grids has been placed too distal respect muscle position, indeed last 2 channels of each column in figure 4.15 (b) show a lower activation.

During this second experiment many trouble has been encountered with cables contact. As a results of this contact, several spikes appeared on emg trace, this case spike is not on the burst of interest but is not always so. This could be a problem for the algorithm, therefore bipolar channels displaying high spikes are considered as bad channels. As far as concern vastus medialis, it shows a lower activity respect to vastus lateralis, particularly concentrated in medial zone. As discuss in advance, biceps femoris is responsible for leg flexion, but in second experiment of this subject, channels selected in this grid seem belonging to semitendinosus. Green rectangle is used in 4.15 (c) to distinguish activation of semitensinosus from biceps femoris. The presence of semitendinosus is due to the large dimension of the electrode grid (8x8 monopolar emg). Biceps femoris shows activation between second 18 till the end of the task, but also between about second 5 and 15. In this interval of time this muscle should not work during extension, probably it is due to cocontraction.

In conclusion, as presented through figure 4.12 (b) and 4.14 (b) not all muscles are necessary to decode movement, in details for ankle are enough 2 out of 3 and for knee 2 out of 4 muscles. This is what happen for subject 3, but also for the other subjects except one. In this last case, for 3 channels configuration all muscles of ankle are considered (1 channels on every muscle) even if for knee is confirmed the previous situation.

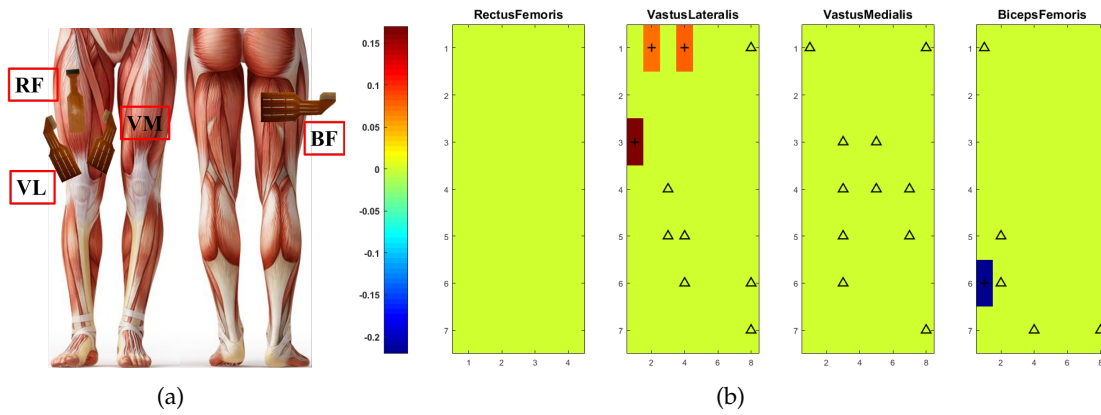
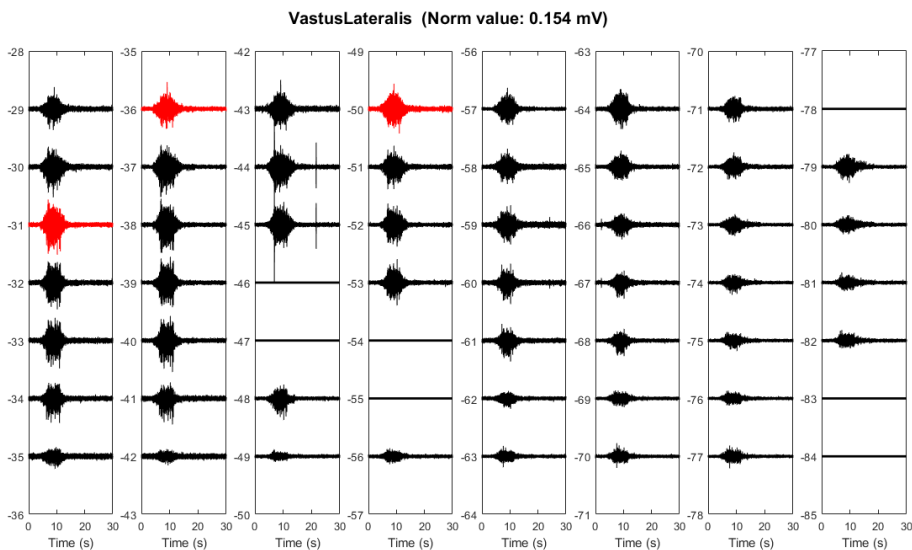
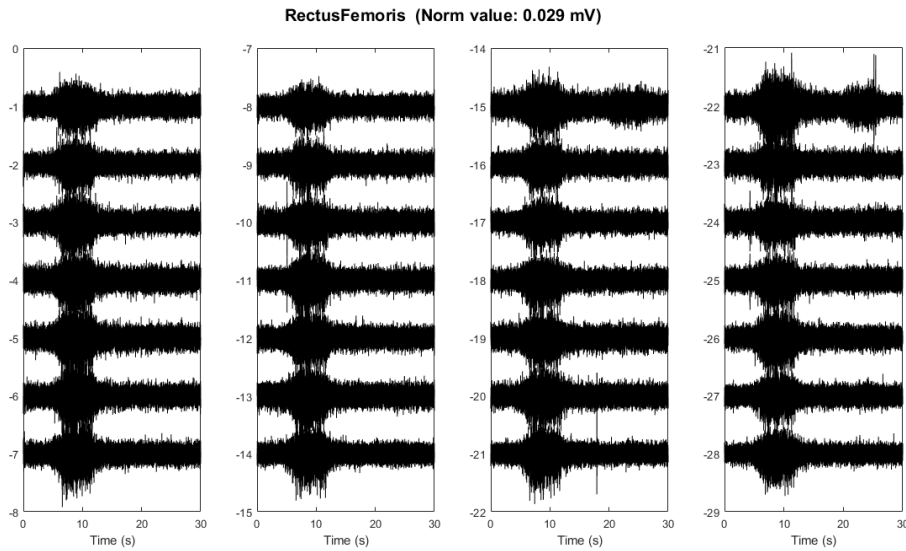
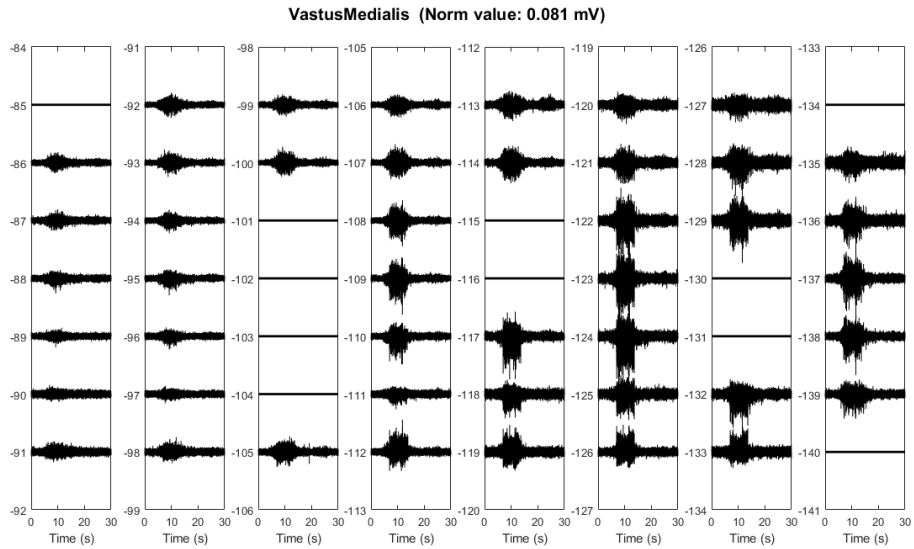
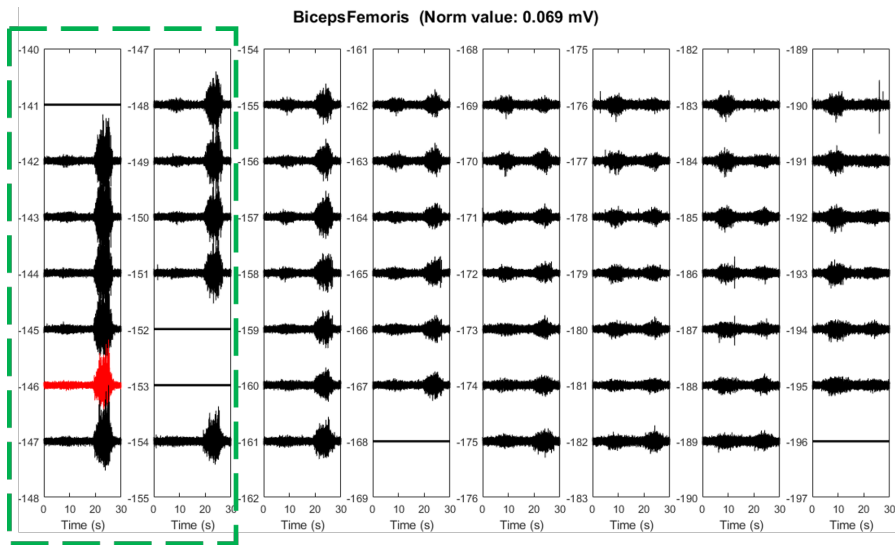


FIGURE 4.14: (b) Colormaps show channels selected for 4-channels configuration and their associated weights. Electrodes grids placement on knee muscles has been reported in (a) to explain colormaps orientation. The order of channels displayed in the colormaps is the same as looking grids applied to the skin of the subject. Data are derived from subject 3.





(c)



(d)

FIGURE 4.15: *Emg bipolar signals of (a) rectus femoris, (b) vastus lateralis, (c) vastus medialis and (d) biceps femoris of subject 3 trial 4. Channels selected by Lasso are colored by red and bad channels were substituted by horizontal black line.*

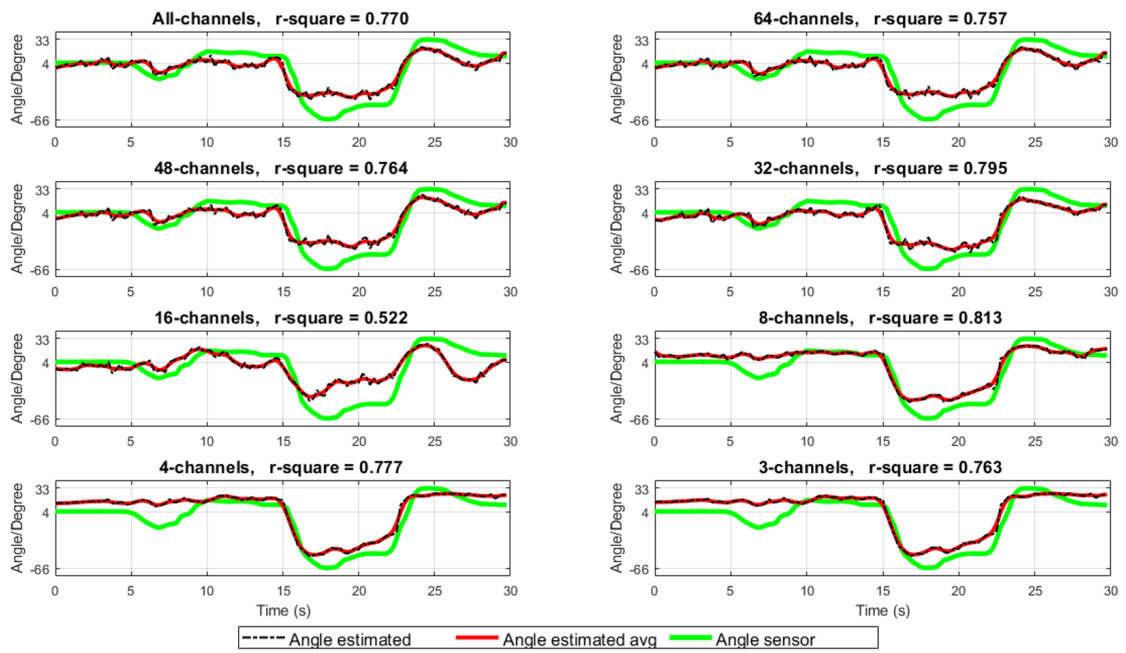
4.2 Second experiment results: angle reconstruction

In this section, angles signals reconstructed from both joints of two subjects are illustrated. A comparison of reconstruction obtained using 10 trial LOOCV method and 5 trials LOOCV has been proposed. Each graphic has on x-axis the time duration of the experiment and on y-axis the angular range. Superior and inferior limits displayed on y-axis depend on the recording provided by electrogoniometers. Same extreme values of each joint were chosen by literature for all subjects in the first experiment, instead in the second experiment they were derived from sensor recording affected with offset, as described in 3.1.2, and misplacements of the sensors. For these reasons, angular ranges of each joint are slightly different among all subjects and also from values used in first part of the study. For example in the first experiment angular range of ankle was between 30 and -50 degree, in the graphics reported for subject 3 in figure 4.17 and for subject 5 in figure 4.16 angular range are between 28 and -60 degree and between 33 and -66 degree, respectively. Above each graphic the number of channels selected in that specific configuration and the r^2 values representing the reconstruction accuracy are reported. In order to verify the angles reconstructions, angles signals related to same trial were estimated using all subsets available. Each graphic shows angle signals recorded by electrogoniometers (green line) and estimated angles signals (dashed black line). An additional red line is drawn, this line represents the estimated angles filtered with a moving average filter. The decision to filter the estimation arrived from a first analysis of the signals reconstructed, the filtering is done in order to obtain smoother control signals. Indeed, the decoded angles signals are almost smooth but in some portion they can manifest very high spike that have nothing to do with angular trend. These spikes are due to contact between cables during the second part of experiment as shown in figure 4.15 (b) about vastus lateralis. Referring to figure 4.18 (a) and (b) the disturb localized at about second 25 is attenuated by filtering (see difference between dashed black line and red line). Moreover, the presence of this spike decreased as the number of electrodes is reduced. Not only, but also for this reason the reconstruction performances expressed by r^2 are higher for subsets with a lower number of channels respect to subsets with an enormous number of electrodes (see 4-channels subset and complete configuration in figure 4.18 (a) and (b)). Probably because disturbs are located on specific channels that are discarded across channel subsets selection.

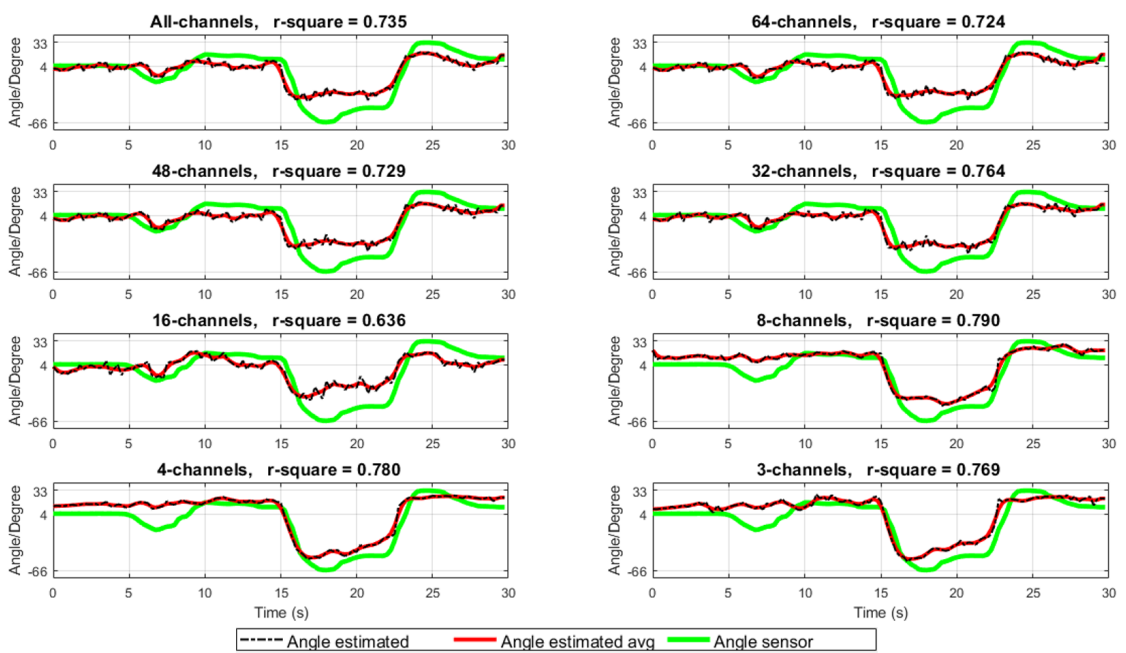
4.2.1 Ankle

Subject 5 shows constant values of performances about decoding ankle angles (figure 4.16 (a) and (b)), on the whole are lower than those of subject 3. Reducing in number of electrodes implies not necessarily a monotonic increase or decrease in performances, as demonstrated in figure 4.16 (a) with 16-channels configuration. r^2 values are particularly below on average, best differences can be appreciated in second half of the task since second 15. This occurs probably because weights associated to one or more channels are not suitable, or rather weights found in first experiment for this channels are not suitable for this task of second experiment. In particular, this situation can occur about ankle joint, because condition in which task has been performed in first and second experiment are quite different. Moreover, about 8, 4 and 3-channels subsets can see that estimated angles are not able to follow closely signals provided by sensor also in first part of the task. The causes are potentially two: a small number of channels is not enough to decode angles of the ankle of this subject or weights associated to them are not suitable.

Different situation can be appreciated analyzing angles reconstructions for ankle joint of subject 3, in figure 4.17 (a) and (b). It figures out that signals were estimated better with a restricted number of electrodes, as indicated by r^2 values. In contrast with data of the previous subject, limited number of channels is enough to follow almost closely angular trend provided by sensor. This behavior matched for both method tested: 10 trials LOOCV and 5 trials LOOCV. Regardless the number of trials is reduced by half, for this subject performances are comparable between these two methods. It means that angles decoding can be obtained with a reduct number of trials.

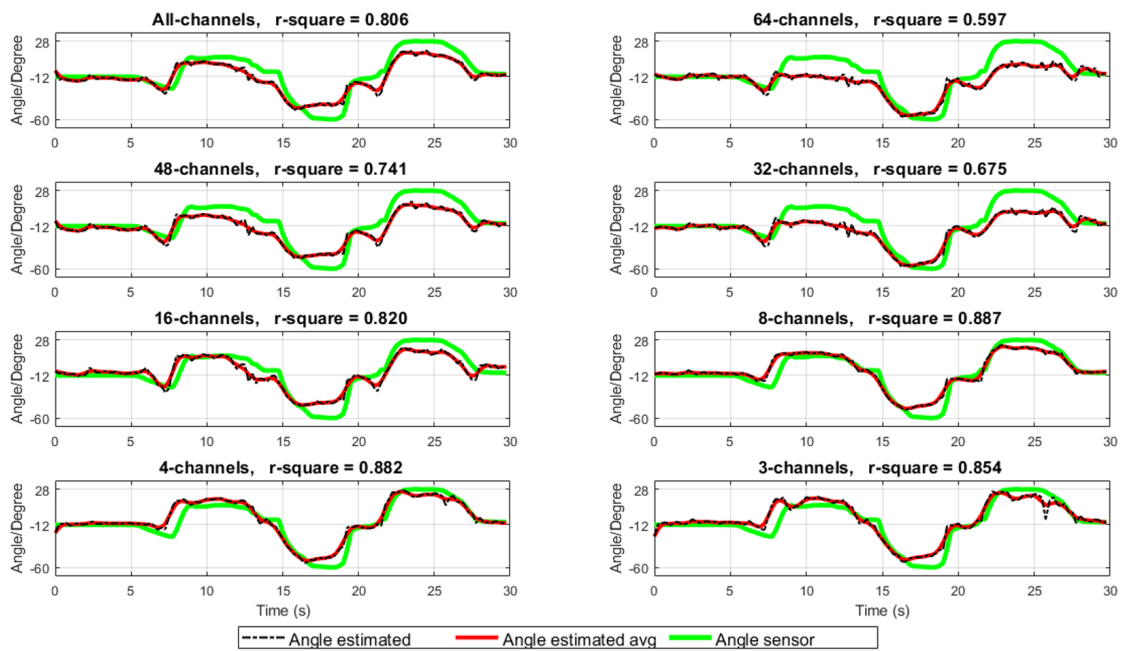


(a)

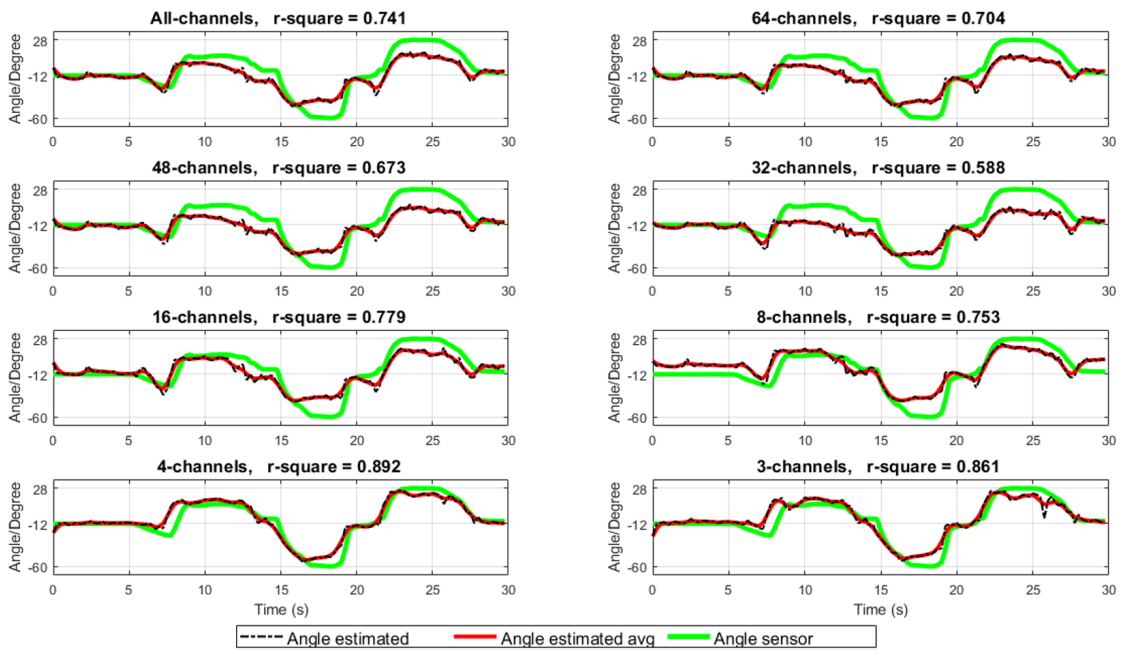


(b)

FIGURE 4.16: Green line represents ankle signal provided by electrogoniometer, dashed black line is the angle estimation and red line is angle estimation filtered using moving average filter. Each graphic shows reconstruction for trial 3 of subject 5 with each subset. Data from 10 trials LOOCV were used in (a) and 5 trials LOOCV in (b).



(a)



(b)

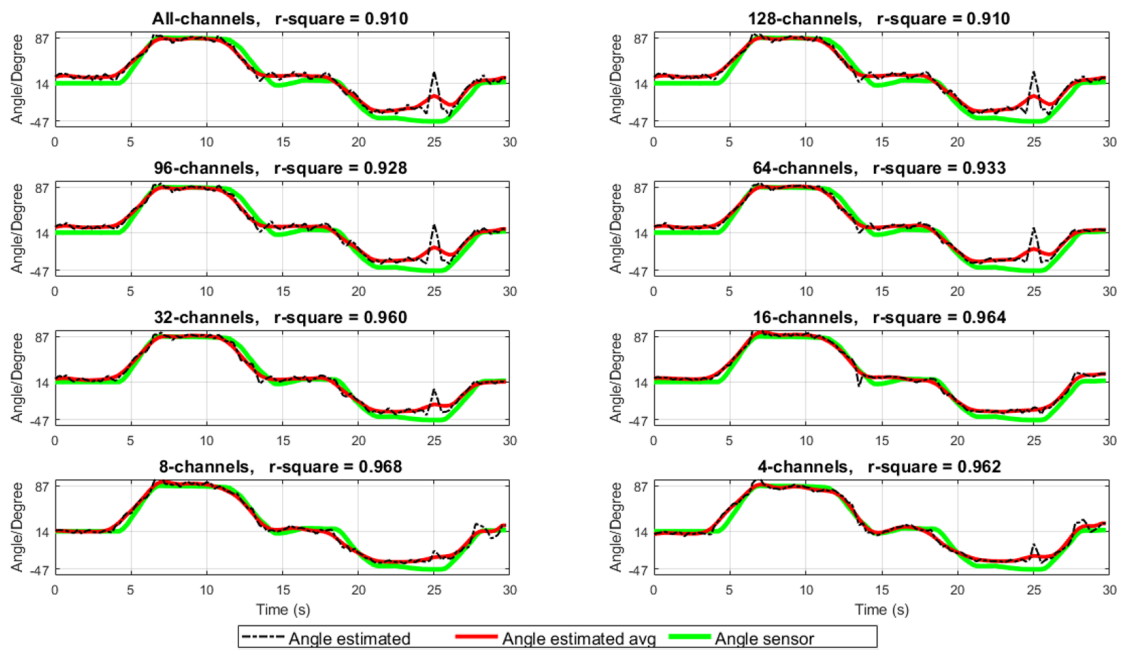
FIGURE 4.17: Green line represents ankle signal provided by electrogoniometer, dashed black line is the angle estimation and red line is angle estimation filtered using moving average filter. Each graphic shows reconstruction for trial 4 of subject 3 with each subset. Data from 10 trials LOOCV were used in (a) and 5 trials LOOCV in (b).

4.2.2 Knee

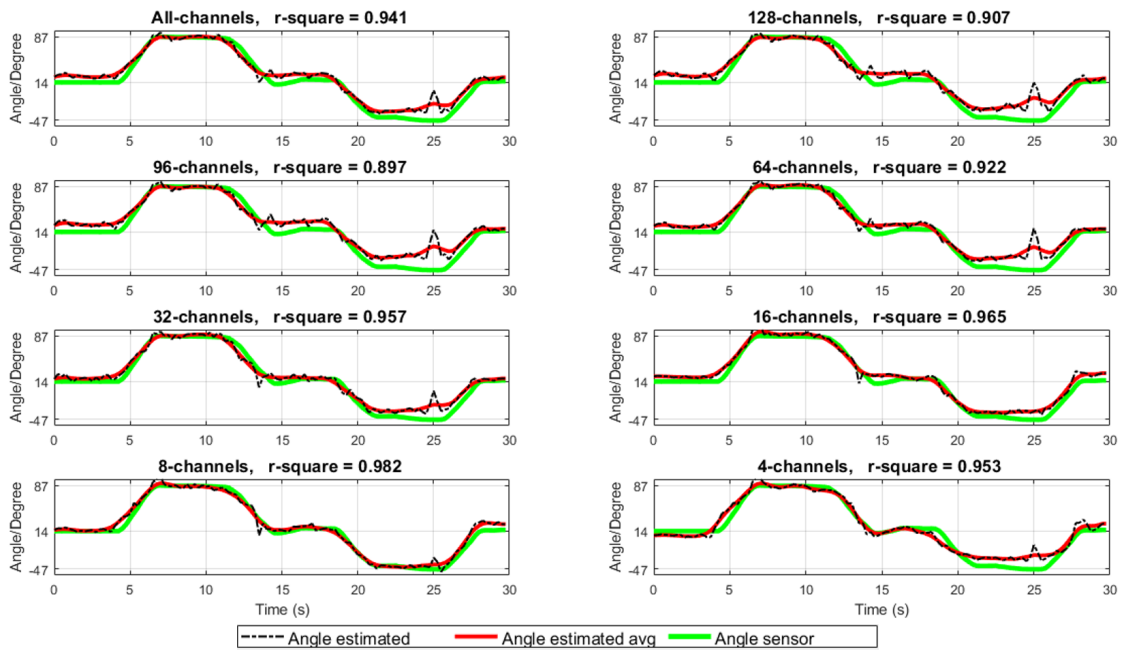
About data of knee joint of subject 5 can be seen that performances in reconstruction are high, moreover they increased as number of electrodes is decreased. Probably, redundancy information complicate decoding phase, sometimes decreasing the accuracy performances. As touched upon at the beginning of the section, the presence of the spike is attenuated reducing number of channels and optimizing the weights. Indeed, for method applied in figure 4.18 (a) has been verified that channels selected in 4-channels subset are included in 8-channels configuration but they are complete different to channels chosen in 16-channels configuration. It means that the presence of that spike is related to a specific channels affected by contact between cables during task.

For what concern knee joint of subject 3 (figure 4.19 (a) and (b)), performances kept constant even if number of channels is reduced, this has value for both methods. There is no differences between results obtained for knee joint with two different number of trials. For both methods, angles reconstructed can follow angles provided by sensor with great accuracy, regardless number of channels involved.

As result of discussion through figure 4.16-4.19, can be appreciated that generally angles signals decoded for ankle have lower accuracy performances than those reconstructed for knee joint. This occurs regardless subject and method, but what figures out is that same performances in reconstruction of angles for both joints can be achieved using only 5 trials, this allows to halve the time of the experiment.

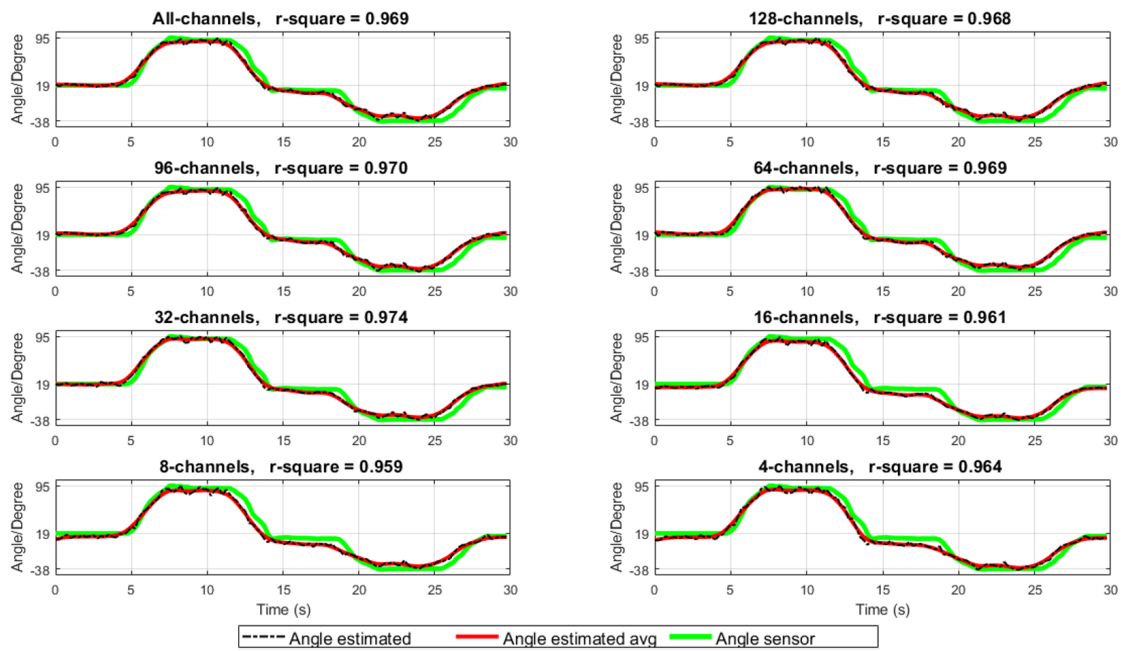


(a)

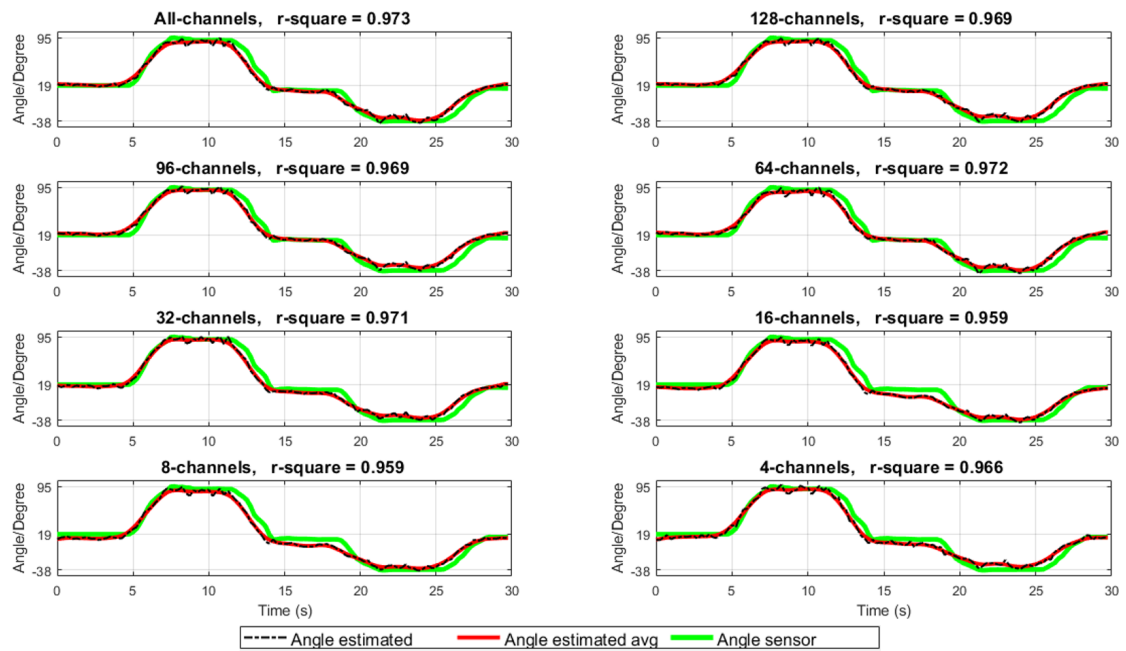


(b)

FIGURE 4.18: Green line represents knee signal provided by electrogoniometer, dashed black line is the angle estimation and red line is angle estimation filtered using moving average filter. Each graphic shows reconstruction for trial 3 of subject 5 with each subset. Data from 10 trials LOOCV were used in (a) and 5 trials LOOCV in (b).



(a)



(b)

FIGURE 4.19: Green line represents knee signal provided by electrogoniometer, dashed black line is the angle estimation and red line is angle estimation filtered using moving average filter. Each graphic shows reconstruction for trial 4 of subject 3 with each subset. Data from 10 trials LOOCV were used in (a) and 5 trials LOOCV in (b).

4.2.3 Statistical analysis

Statistical analysis has been conducted to check what factors influenced the channel selection method proposed in this study. For this reason three-way ANOVA has been performed to evaluate the dependence of algorithm performances from 3 main factors: subjects, channel subsets, and joint of interest (ankle and knee). Channel subsets means the eight subsets defined for ankle and knee joint (table 3.1). To evaluate performances r^2 and $rmse$ values has been used in two separated analysis. In details, data set used for every subject depends on type of cross validation used, for this reason this evaluation has been performed for 10 trials LOOCV and 5 trials LOOCV hence the data set of movements, for each subject, was made of 10 and 5 movements, respectively. For this reason three-way ANOVA was performed 4 times. In table 4.1 it can be observed that same results were obtained regardless the reduced number of trials. Channel selection method proposed in this study is strongly influenced by subjects and joints, but in the same way it is strongly independent by number of channels that defined a subset. In other words, this approach is patient specific, or rather depends on physiological and anatomical characteristics of the subject. It means that, unfortunately, this approach can be not generalized for every patient: channels selected depend on subject, but it is not influenced by number of channels request.

	10 Trials LOOCV		5 Trials LOOCV	
	r^2	$rmse$	r^2	$rmse$
subjects	$p<0.05$	$p<0.05$	$p<0.05$	$p<0.05$
subsets	NS	NS	NS	NS
joints	$p<0.05$	$p<0.05$	$p<0.05$	$p<0.05$

TABLE 4.1: Table reports p values related to four analysis evaluated with three-way ANOVA: first two columns are related to performances metric extracted by 10 trials LOOCV, instead the last two columns are related to 5 trials LOOCV and its performances results. Factor subjects depends on the cross validation: number of patients are always five, but number of trials associated to them depends on choice of method.

Chapter 5

Conclusion

In this study channel selection method was examined to prove its robustness for the extraction of a lower limb exoskeleton control signal based on regression technique. The proposed approach allows to determine optimal position of a specific number of electrodes with high density sEMG recording to provide angular control signals. For this reason, the feasibility to reconstruct angle signals using a small number of electrodes has been demonstrated. In particular has been proved that this approach is suitable for able-body healthy subjects also without using angle sensors. Generally, these type of sensor request time to be positioned accurately and to be calibrated for each specific subject. Moreover, since most of exoskeleton structure are bulky, the placement of many electrodes grids and external sensors could be not suitable.

The drawback of this approach is that it depends on the movements performed in first experiment: angular range of task in second experiment movements have to be included in angular range of those of first experiment. Indeed, it is important to highlight that trapezoidal cues of first experiment used to perform effective channel selection were created for healthy able-bodied patient. This way these trajectories need to be conformed to the subject physiological characteristics in case of a pathological patient. In particular, angular range (maximum and minimum values) for each joint needs to be measured manually on subject and then trajectories can be modeled on his proper angular range. This because is fundamental that subject follows the cue as best he can in order to achieve a valid channels selection.

In second experiment performances related to knee joint were higher than those obtained for ankle joint. Probably, because movements for first and second experiment were more similar for knee than for the ankle. Indeed, for future experiments this is an aspect to improve in order to enhance performances on ankle. Considering all robustness test results and reconstruction performances, it is possible to use this approach with a reduced number of trial to select most informative channels, this aspect allows to save time in term of clinical use.

In terms of clinical use, computational time to select channels and find their weights was taken into account. Algorithm employed less than ten minutes to select a channel subset for knee, and less than 5 minutes for ankle. Time difference between joints depends on number of channels placed. On the other hand, many challenges needed to be overcome before experimental setup described in this study became suitable for a clinical use. Encumbrance and interferences provided by cables are the main problems which can be resolved, for example, with bluetooth technologies. Also, experimental setup requires much time that has to be reduced in order to make this protocol suitable for clinical application.

In this preliminary study, the proposed approach has been evaluated only offline, moreover angles and emg signals information were evaluated, but to improve this approach muscle force estimation has to be taken into account. In this work, subjects performed the experiments without wearing exoskeleton, hence in a future experiment the feasibility of this protocol has to be tested in a complete experiment where subject wears exoskeleton frame. Moreover because different levels of force can be recorded from muscles to reach same angles position. How to combine angle and force information is one of the main aspects to examine in future works.

The aim behind this approach was to individuate the most informative areas of muscular region and hence to reduce number of channels that best allow to generate a robust angular control signal. In terms of clinical use, this protocol has been designed to be applied once in a rehabilitation process. Successively, a limited number of electrodes will be applied only in positions of interest found for every muscle in the first application. In conclusion, analysis results of this study showed that generally reconstruction performances obtained with complete configurations of electrodes can be achieved and also overcome with a lower number of channels, most of cases with the smallest subset of channels. Hence, this work provides evidence of feasibility to extract a robust control signal for a proportional myoelectric control with a limited number of electrodes located on the most informative regions of muscle.

Bibliography

- [1] Antonio J del-Ama et al. “Hybrid FES-robot cooperative control of ambulatory gait rehabilitation exoskeleton”. In: *Journal of neuroengineering and rehabilitation* 11.1 (2014), p. 27.
- [2] Bradley Efron et al. “Least angle regression”. In: *The Annals of statistics* 32.2 (2004), pp. 407–499.
- [3] PEng Erik Scheme MSc and PEng Kevin Englehart PhD. “Electromyogram pattern recognition for control of powered upper-limb prostheses: State of the art and challenges for clinical use”. In: *Journal of rehabilitation research and development* 48.6 (2011), p. 643.
- [4] Anders Fougner et al. “Control of upper limb prostheses: terminology and proportional myoelectric control—a review”. In: *IEEE Transactions on neural systems and rehabilitation engineering* 20.5 (2012), pp. 663–677.
- [5] Janne M Hahne et al. “Linear and nonlinear regression techniques for simultaneous and proportional myoelectric control”. In: *IEEE Transactions on Neural Systems and Rehabilitation Engineering* 22.2 (2014), pp. 269–279.
- [6] JM Hahne et al. “Simultaneous and proportional control of 2D wrist movements with myoelectric signals”. In: *Machine Learning for Signal Processing (MLSP), 2012 IEEE International Workshop on*. IEEE. 2012, pp. 1–6.
- [7] He Huang et al. “An analysis of EMG electrode configuration for targeted muscle reinnervation based neural machine interface”. In: *IEEE Transactions on Neural Systems and Rehabilitation Engineering* 16.1 (2008), pp. 37–45.
- [8] Han-Jeong Hwang, Janne Mathias Hahne, and Klaus-Robert Müller. “Channel selection for simultaneous and proportional myoelectric prosthesis control of multiple degrees-of-freedom”. In: *Journal of neural engineering* 11.5 (2014), p. 056008.
- [9] Han-Jeong Hwang, Janne Mathias Hahne, and Klaus-Robert Müller. “Channel selection for simultaneous myoelectric prosthesis control”. In: *Brain-Computer Interface (BCI), 2014 International Winter Workshop on*. IEEE. 2014, pp. 1–4.

-
- [10] Ning Jiang et al. "EMG-based simultaneous and proportional estimation of wrist/hand kinematics in uni-lateral trans-radial amputees". In: *Journal of neuroengineering and rehabilitation* 9.1 (2012), p. 42.
- [11] Ning Jiang et al. "Myoelectric control of artificial limbs—is there a need to change focus?[In the spotlight]". In: *IEEE Signal Processing Magazine* 29.5 (2012), pp. 152–150.
- [12] Kalypso Karastergiou et al. "Sex differences in human adipose tissues—the biology of pear shape". In: *Biology of sex differences* 3.1 (2012), p. 13.
- [13] Roberto Merletti, Philip A Parker, and Philip J Parker. *Electromyography: physiology, engineering, and non-invasive applications*. Vol. 11. John Wiley & Sons, 2004.
- [14] Silvia Muceli and Dario Farina. "Simultaneous and proportional estimation of hand kinematics from EMG during mirrored movements at multiple degrees-of-freedom". In: *IEEE transactions on neural systems and rehabilitation engineering* 20.3 (2012), pp. 371–378.
- [15] Robert Tibshirani. "Regression shrinkage and selection via the lasso". In: *Journal of the Royal Statistical Society. Series B (Methodological)* (1996), pp. 267–288.
- [16] MK Vijaymeena and K Kavitha. "A survey on similarity measures in text mining". In: *Machine Learning and Applications: An International Journal* 3.2 (2016), pp. 19–28.